Calhoun: The NPS Institutional Archive

DSpace Repository

Theses and Dissertations 1. Thesis and Dissertation Collection, all items

1967-08

A high enthaply [i.e., enthalpy] test facility powered by a gaseous core reactor.

Flynn, Noel Steven

Cambridge, Massachusetts; Massachusetts Institute of Technology

http://hdl.handle.net/10945/12285

Downloaded from NPS Archive: Calhoun

Calhoun is the Naval Postgraduate School's public access digital repository for research materials and institutional publications created by the NPS community. Calhoun is named for Professor of Mathematics Guy K. Calhoun, NPS's first appointed -- and published -- scholarly author.

Dudley Knox Library / Naval Postgraduate School
411 Dyer Road / 1 University Circle
Monterey, California USA 93943

http://www.nps.edu/library

NPS ARCHIVE
1967
FLYNN, N.

hesis
527

A HIGH ENTHAPLY TEST FACILITY
POWERED BY A GASEOUS CORE
REACTOR

by

Noel Steven Flynn, Lieutenant, U.S. Navy
B.S. United States Naval Academy (1959)

SUBMITTED IN PARTIAL FULFILLMENT ON THE
REQUIREMENTS FOR THE DEGREES OF MASTER
OF SCIENCE AND ENGINEER OF AERONAUTICS
AND ASTRONAUTICS

at the

MASSACHUSETTS INSTITUTE OF TECHNOLOGY

967
FLYNN, N.

NAVAL POSTGRADUATE SCHOOL
MONTEREY, CALIF. 93940

A HIGH ENTHALPY TEST FACILITY
POWERED BY
A GASEOUS CORE REACTOR

by

Noel Steven Flynn

Submitted to the Department of Aeronautics and Astronautics on 21 August 1967 in partial fulfillment of the requirements for the degree of Master of Science and Engineer of Aeronautics and Astronautics.

ABSTRACT

The feasibility of utilizing a gaseous core nuclear reactor to provide high enthalpy, high pressure gas flow for simulating atmospheric re-entry conditions was investigated. The test facility uses a mixture of nitrogen and uranium in a closed cycle with no attempt to contain the uranium fuel within the core. The primary purpose of the facility is to provide high enthalpy, high shear flows for testing re-entry materials and shapes.

Investigated in this study were the effects of the nitrogen-uranium mixture on reactor criticality, nuclear contamination of the test model, protection of the reactor core and nozzle structure from imposed heat loads and operating limitations of the test facility.

Thesis Supervisor: W. Stephen Lewellen

Title: Associate Professor of
Aeronautics and Astronautics

ACKNOWLEDGEMENTS

The author wishes to express his appreciation to the following persons: Associate Professor W.S. Lewellen, who, as thesis advisor provided the encouragement, advice and direction necessary in this type of effort ; and Miss Germaine Lessard, who typed the manuscript.

Acknowledgement is made to the Department of the Navy, and to the United States Naval Postgraduate School, Monterey, California, who made this work possible.

TABLE OF CONTENTS

Chapter No.		Page No.
	Introduction	1-3
I	Re-Entry Conditions	4-12
1.1	Pressure and Enthalpy	4
1.2	Power Requirements	8
1.3	Test Time	10
1.4	Existing Facilities	10
II	Test Facility	13-17
2.1	Gaseous Core Reactor Requirements	13
2.2	Gas Cycle	14
2.3	Component Interface Problems	17
III	Gaseous Core Neutronics	18-27
3.1	General	18
3.2	Criticality Condition	19
IV	Model Nuclear Contamination	28-40
4.1	Radiation Damage	28
4.2	Biological Hazards	30
4.2a	Contamination Environment	30
4.2b	Model Contamination	37

Chapter No.		Page No.
V	Reactor Cooling	41-47
5.1	Heat Loads	41
5.2	Criticality Effects	42
5.3	Reactor Flow Pattern	43
5.4	Radiation Barrier	44
5.5	Moderator Cooling	46
VI	Nozzle Heat Transfer	48-60
6.1	Nozzle Size	48
6.2	Heat Loads	48
6.3	Nozzle Configuration	49
6.4	Maximum Heat Transfer	50
6.5	Material Selection	51
6.6	Test Section Mach Number	53
6.6	Transpiration Cooling Requirements	54
VII	Auxiliary Equipment	61-68
7.1	General	61
7.2	Water Diffusor	61
7.3	Fuel Separator	63
7.4	Turbines and Pumps	64
7.5	Minimum Power Level	66
VIII	Conclusions	69-71
Table I	Fission Products	72

Figure Page No.

1 Re-Entry Stagnation Pressure and Enthalpy 73
2 Re-Entry Simulation Power Requirements 74
3 Test Facility Schematic 75
4 Nitrogen Cycle 76
5 Water Cycle 77
6 Criticality of Bare Uranium-Nitrogen Gaseous Reactor 78
7 Critical Radius of Beryllium Reflected Uranium-Nitrogen Gaseous Reactor 79
8 Nozzle Heat Loads 80
9 Transpiration Cooling Requirement 81
10 Nozzle Transpiration Flow 82
11 Minimum Operating Power for Gaseous Core Reactor 83

References 84-86

SYMBOLS

$\mathcal{A}$	Avogadro's number, 6.023×10^{23} molecules/gram mole
A	area, centimeters^2
	atomic number, species
B	buckling, centimeters^{-1}
C	coefficient
	constant
D	diameter, centimeters
E	modulus of elasticity, kilograms/millimeter, pounds-force/inch^2
F	blowing parameter[11]
G	transpiration cooling mass velocity[11]
H	enthalpy, gram-caleries/gram
K	earth gravitational constant, 4×10^{14} meter^3/second^2.
$\mathcal{L}$	neutron diffusion time, seconds
L	diffusion length, centimeters
	length, centimeters
$\mathcal{M}$	molecular weight, grams/gram-mole
N	number density, particles/centimeter^3
P	pressure, absolute atmospheres
$\mathbb{P}$	power, megawatts
Q	heat flux, gram-caleries/centimeter^2-second
R	radius, centimeters
S	reflecter saving, centimeters
T	temperature, °Kelvin

V	velocity, centimeters/second
V_{ol}	volume, centimeters^3
W	work, megawatts
Z	compressibility
c	speed of sound, centimeter/second
d	thickness, centimeters
e	thermal absorptivity
g	acceleration constant, 980.7 centimeter/second^2
h	coefficient of convective heat transfer, caleries/centimeter^2 - sec - ° Kelvin
k	thermal conductivity, caleries/centimeter - °Kelvin
	Boltzmann's constant, 1.3805 x 10^{-16} ergs/°Kelvin
	multiplication factor
m	mass flow rate, grams/second
p	pressure differential, atmospheres
r	radius, centimeters
t	time, seconds
v	neutron velocity, meter/seconds
x	axial distance from nozzle throat, centimeters
y	altitude, nautical miles
α	coefficient of linear expansion centimeter/ centimeter-°Kelvin
	density proportionality constant[1], 0.715
β	density exponential constant[1], 1/7.3 x 10^{3}meters
γ	ratio of specific heats
δ	extrapolation distance, centimeters
ϵ	energy per fission, megawatt-sec/fission
	absorptivity
ξ	mole fraction
η	fission fragment fraction

θ	angle, radians
κ	mean radiation absorption coefficients, cm^{1}
λ	decay constant
	mean free path, centimeters
μ	viscosity, gram/second-centimeter
ν	neutron fission multiplication factor
ρ	density. grams/centimeter^{3}
σ	stress, kilograms/millimeter, pounds-force/inch^{2}
	Stepfan-Boltzman constant, 5.67×10^{-5} erg/ cm^{2} - ^{o}Kelvin - sec
ϕ	neutron flux, neutrons/centimeter^{2} - second
ω	temperature-Mach number correction exponent[10]
	angular velocity, radians/second
Σ	macroscopic cross section, centimeters^{-1}
δk	reactivity
$t_{1/2}$	half life, seconds
∞	infinity

Subscripts

a	absorption
aw	adiabatic wall
e	entry body
c	core
	coolant
	carbon
d	delayed
δk	reactivity
eff	effective
f	fission
	flight

f	fuel
g	geometric
h	hoop (stress)
m	material
	model
	moderator
N	nitrogen
o	orginal
r	radiation
	reflector
rej	rejected
s	scatter
	streaming
	seed
	saturation
t	coolant tube
th	thermal
tr	transpiration
	transport
w	wall, hot side
wo	wall, cold side
u	uranium
	ultimate
0	stagnation
$1, 2, \ldots$	station numbers
$-$	average
∞	infinite

INTRODUCTION

Many problems areas have been uncovered and investigated in our attempt to master space. One area is the re-entry of a ballistic, orbital or superorbital body into a planetery atmosphere and the delivery of an payload to the planet's surface.

The kinetic and potential energy of the body must be dissipated to insure successful payload delivery. Atmospheric braking, with the transfer of energy from the high velocity re-entry body to the surrounding air, is often the optimum entry system.[1]

The body must be protected from the high heat loads due to friction and the rapid compression heating of the air immediately surrounding the body. Ablative materials are used to both protect the body, by acting as an insulator, and to carry away the heat that is absorbed by the ejection of mass of the ablative material.[2]

The ablative process, however, is very complex and attempts to analytically predict the behavior of new materials and shapes have met with little success.[3] Various attempts at simulating re-entry conditions have been made, but no existing facility can completely duplicate the

re-entry environment, although some aspects of the problem can be simulated.[4,5]

Existing test facilities cannot duplicate the high enthalpy, high shear regime for a sufficiently long test time to be able to investigate this critical ablation region.[3]

This study will investigate the feasibility of a high enthalpy test facility which uses a fissionable gas reactor as a power source. The gas core reactor drives a closed cycle test system and provides the necessary energy for high enthalpy, high pressure gas flows of long duration.

In establishing the feasibility of this system, the re-entry problem is first investigated to establish the power requirements of the system.

Stagnation pressure and enthalpy are determined by the method outlined in Reference 1, from these the power required to simulate an atmospheric entry in a ground test facility is determined.

Then the reactor itself is studied. The gaseous core reactor utilized is similar in operating principle to the gaseous core nuclear rocket engine proposed as the next generation space booster.[6,7,8] However, as the proposed system incorporates a closed operating cycle, containment of the nuclear fuel does not present an obstacle as it does in the gaseous core nuclear rocket. Critical size, fuel concentration and fuel-nitrogen ratio, where nitrogen is the working fluid, are determined using the

diffusion approximation and one group neutron theory.[9] The contamination problems associated with the utilization of a nuclear medium are also investigated.

The combined heat loads to the reactor and nozzle are examined. The heat loads in the nozzle are determined[10] and homogenous transpiration cooling[11] to protect the nozzle is examined. The use of a seeded carbon particle layer to protect the moderator from radiation heat loads is also examined.[12, 13]

Finally the power requirements of auxiliary equipment to maintain steady state closed cycle operation are examined.

CHAPTER I

RE-ENTRY CONDITIONS

1.1 Pressure and Enthalpy

To test the materials used in a re-entry vehicle it is necessary to know the velocity, the pressure and the heating involved in the re-entry.

As a typical example consider a vehicle returning to earth with a superorbital velocity. An estimate of the velocity can be obtained by assuming it equal to the velocity needed to escape from a nonrotating earth, with no drag forces. The energy per unit mass to escape from the earth, acting as a central force field is

$$\frac{1}{2}V_e^2 = \frac{k}{R} \tag{1.1}$$

and the velocity to escape is

$$V_e = \sqrt{\frac{2k}{R}} \tag{1.2}$$

when k is the earth gravitational constant, 4×10^{14} $^{m}/_{sec^2}$ and R is the earth's radius, 6.4×10^{6} m. , the escape

velocity from the earth's surface is 1.12×10^4 m/sec.

This is the minimum for earth escape and is the minimum at which a superorbital body will approach the sensible atmosphere, commencing re-entry.

Expressions for stagnation pressure and enthalpy, at the point of maximum pressure and also at the point of maximum heating rate, may be found by using the velocity altitude history given in Reference 1 for an exponential atmosphere,

$$V = V_e\, e^{\left\{\frac{-C_D A}{2m \sin\theta_e} \quad \frac{\rho_o \alpha e^{-\beta y}}{\beta}\right\}} \tag{1.3}$$

where V_e is the initial entry velocity, C_D is the coefficient of drag of the body, m the mass of the body, θ_e the entry angle and α and β are constants defined by

$$\rho = \rho_o \alpha e^{-\beta y} \tag{1.4}$$

The stagnation pressure on the body is approximated by Newtonian theory with the body angle considered small and the ambient pressure neglected. The stagnation pressure at any point in the entry is

$$P_o = \rho_o \alpha e^{-\beta y} V_e^2 \exp\left(\frac{-C_D A}{m \sin\theta_e} \quad \frac{\rho_o \alpha e^{-\beta y}}{\beta}\right) \tag{1.5}$$

For maximum stagnation pressure, set $\frac{dP_o}{dy} = 0$ and obtain

$$\frac{dP_o}{dy} = C_1 e^{-\beta y}(-\beta) e^{C_2 e^{-\beta y}} + C_1 e^{-\beta y} e^{C_2 e^{-\beta y}} C_2 e^{-\beta y} - (-\beta) = 0 \qquad (1.6)$$

where

$$C_1 \equiv \rho_o \alpha V_e^2$$

$$C_2 \equiv -\frac{C_D A}{m \sin\theta_e} \qquad \frac{\alpha \rho_o}{\beta}$$

C_1 and C_2 are fixed by the atmospheric model ballistic parameter, $\frac{C_D A}{m \sin\theta_e}$, and initial entry velocity; and remain constant during re-entry.

The altitude for maximum stagnation pressure during re-entry is given by

$$y = \frac{1}{\beta} \ln \frac{C_D A}{m \sin\theta_e} \qquad \frac{\alpha \rho_o}{\beta} \qquad (1.7)$$

Since the velocity for maximum stagnation pressure is given by

$$V = V_e e^{-\frac{1}{2}} \qquad (1.8)$$

and associated density is

$$\rho = \frac{m \sin\theta_e}{C_D A} \beta \qquad (1.9)$$

the maximum stagnation pressure is

$$P_{o_{MAX}} = \frac{m \sin\theta_e}{C_D A} \qquad \frac{\beta V_e}{e} \qquad (1.10)$$

and the stagnation enthalpy is

$$H_o = h + \frac{V^2}{2} \qquad (1.11a)$$

or since the static enthaply is very much less than dynamic enthalpy,

$$H_o \cong \frac{V_e^2}{2e} \qquad (1.11b)$$

Similarly, expressions are obtained for stagnation pressure and enthalpy at the point of maximum rate of convection heating of the stagnation point, where stagnation point heating rate is given by[1]

$$\frac{dH_o}{dt} = C_s \sqrt{\frac{\rho}{\sigma}}\; V^3 \qquad (1.12)$$

where C_s is the stagnation point coefficient of heat transfer, a function of body configuration, σ is the radius of curvature at the stagnation point, and ρ and V are functions of altitude. To obtain the point of maximum stagnation point heating rate, the previously derived expressions for ρ and V are substituted in the above.

For the maximum set $\frac{d}{dy}\left(\frac{dH_o}{dt}\right)=0$, obtaining

$$\left.\frac{dH_o}{dt}\right)_{MAX} = C_s \sqrt{\frac{m \sin\theta_e}{C_D A}\;\frac{\beta}{3e\sigma}}\; V_e^3 \qquad (1.13)$$

which occurs at an altitude of

$$y = \frac{1}{\beta} \ln \frac{C_D A}{m \sin\theta_e}\;\frac{\alpha}{\beta} \qquad (1.14)$$

and velocity of

$$V = V_e \; e^{-1/6} \tag{1.15}$$

The associated stagnation pressure is

$$P_o = \frac{m \sin\theta_e}{C_D A} \; \frac{V_e^2 \beta}{3 \, e^{1/3}} \tag{1.16}$$

and stagnation enthalpy is given by

$$H_o = \frac{V_e^2}{2 e^{1/3}} \tag{1.17}$$

Figure 1 shows the extremes of stagnation pressure verses stagnation enthalpy which are encountered during an atmospheric re-entry. The ballistic parameter, $\frac{m \sin\theta_e}{C_D A}$, is a free parameter in determining the envelope. Two envelopes are shown, one for $V_e = 1.12 \times 10^4$ m/sec , corresponding to velocity entering the sensible atmosphere equal to escape velocity. The other is for $V_e = 0.8 \times 10^4$ m/sec, corresponding roughly to 100 n.m. orbital velocity. It can be readily seen in Figure 1 that:

i) stagnation enthalpy at maximum heating rate and maximum stagnation pressure is independant of the ballistic parameter, but increases with increasing initial entry velocity.

ii) stagnation pressure increases directly as entry velocity and directly with ballistic parameter.

1.2 Power Requirements for Simulation

The stagnation pressure on the test model is fixed

by re-entry conditions but the chamber pressure is limited by structural considerations. The maximum chamber pressure is set at 1000 atmospheres for the analysis. It is desirable to test at the lowest possible Mach numbers consistent with representing hypersonic pressure and heating rate distributions. For this reason, and to minimize nozzle losses and cooling requirements, a test Mach number, M_t, of 3.0 is used in this analysis.

For isentropic frozen flow through the nozzle, the power required per unit throat area is

$$\frac{\mathbb{P}}{A_*} = \frac{P_0 H_0}{\sqrt{ZRT_0}} \sqrt{\gamma \left(\frac{2}{\gamma+1} \right)^{\frac{\gamma+1}{\gamma-1}}} \tag{1.18}$$

If Equations 1.16 and 1.17 are used for P_0 and H_0 respectively, the power required per unit throat area to simulate the conditions at the point of maximum heating rate is

$$\frac{\mathbb{P}}{A_*} = \frac{1}{\sqrt{ZRT_0}} \frac{m \sin \theta_e}{C_D A} \frac{V_e^4 \beta}{6 e^{2/3}} \sqrt{\gamma \left(\frac{2}{\gamma+1} \right)^{\frac{\gamma+1}{\gamma-1}}} \tag{1.19}$$

These power requirements are plotted in Figure 2 against initial entry velocity with the ballistic parameter as a free parameter. Reference 14 was used to obtain the characteristics of nitrogen, which was taken as the test gas.

Limiting the chamber pressure to 1000 atmospheres

established one limit on the re-entry profiles that can be simulated. Another is set by limiting the chamber temperature to 10,000°K, this upper limit is set after a consideration of the heat transfer loads experienced in the various test facility components.

1.3 Test Time

The main purpose of this facility is to examine the behavior of re-entry materials and shapes under the high heat and shear loads of an atmospheric re-entry. Such materials are ablative in nature, that is, they absorb heat by increasing in temperature and changing in chemical or physical state. The heat is carried away from the surface by a loss of mass. The departing mass also blocks part of the convective heat transfer to the remaining material.[2] The tunnel running times are set by the time required for the rate of ablation to reach equilibrium. This time is a function of the ablative material[15] and for typical ablative materials[2], such as, graphite and glass reinforced phenolics, the ablative equilibium times is extended to 200 seconds.[4]

1.4 Existing Facilities

Shock tubes are used to generate higher temperatures and pressures to simulate re-entry conditions. The Cornell Aero Laboratory[16] six foot hypersonic tunnel can generate stagnation temperatures and pressures up to 4200°K and 2000 atmospheres respectively. The test time for these pressures however is only 4 micro-seconds. This tunnel can

be upgraded to 10,000°K and 2000 atmospheres but still has a run time far too short to produce the time history of high temperatures and pressures at which the ablative materials fail.

The test time for a shock tube may be increased by using several tubes fired in a Gatling gun fashion. This however only increases run time to seconds, developing a jet power of 25,000 HP[17], about four orders of magnitude too small for re-entry requirements.

High enthalpy and pressure flow is also possible utilizing a hot shot tunnel powered by an electrical discharge arc. This type of tunnel requires large amounts of stored electrical energy and is presently limited to a few hundredths of a second operation.[5]

Although these facilities can approach the desired levels of enthalpy and pressure, they cannot maintain these conditions for a sufficient lenght of time. They are severely power limited. As an example, the power required, from Figure 2, to simulate the re-entry of a vehicle whose ballistic parameter is 2000 grams/ cm^2 and initial entry velocity is 8000 meters/second, is 30 megawatts per cm^2 of throat area. This is about ten percent of the total output of the Grand Coulee Dam for each square centimeter of nozzle throat area.

Plasma arc tunnels provide high enthalpy but low pressure flows and are currently being used to test re-entry materials. These facilities are also power limited and operate at low stagnation pressures and use argon as a working fluid

to achieve long duration tests with comparatively low power inputs.[5]

Because of these high power requirements, a gaseous core reactor is suggested to drive the test facility, the gaseous core because its operating temperature is limited only by heat loads to the containing structure and can operate at the desired temperature, 10,000°K.

CHAPTER II

TEST FACILITY

2.1 Gaseous Core Reactor Requirement

The power required to produce long duration high pressure,high enthalpy gas flows appears to be technically achievable only with nuclear power. Conventional combustion is limited by the recombination of combustion products, which absorb energy and result in an equlibrium temperature far below the required stagnation temperature. In atomic reactors, solid and liquid core operating temperatures have upper limits, the former is the melting point of the nuclear core and, or, structure and the later is boiling point of the liquidized fuel, and, or, melting point of the structure.

A gaseous core nuclear reactor is capable of steady state operation at very high temperatures and pressures. The operating temperature of a nuclear reactor utilizing a fissionable gas core is limited only by the heat load that the hot gas imposes on the container. These heat loads can be controlled to some degree by a combination of convective and transpiration cooling and by injection of a thermal radiation absorber to block radiation heat transfer to the wall. The gaseous core reactor in this study is capable of providing the energy necessary to run a test

at the desired stagnation pressures and enthalpy, that is, 7,100 megawatts.

2.2 Gas Cycle

To simulate the effects of atmospheric heating, nitrogen is used as the working medium. Uranium 235, initially a fine power, is the nuclear fuel. Biological hazards and economic necessity make it mandatory that the uranium fuel be contained within the core of a gas core nuclear rocket.[18] As the proposed system is a closed system, these considerations do not apply. This is not to say, a priori, that fuel containment in the core proper is not required. Presence of uranium in the nitrogen flow complicates the analysis and interpretation of experimental data. If the ratio of mass flow of uranium to nitrogen is limited to a maximum value of ten percent, or about one percent mole ratio, it should permit the assumption that the flow in the nozzle and test section behave as a pure nitrogen flow. This limit is imposed as the maximum allowable uranium content for thermodynamically simulating the effects of atmospheric entry.

The presence of fissionable gas in the closed cycle causes induced radioactivity of the system components. State of the art shielding and radioactive materials handling techniques[9] are assumed sufficient to provide necessary biological protection. As this facility would be very expensive to construct,it is necessary that the induced radioactivity of the model be within biological limits for examination of the model within a short time after

the test and associated radioactive exposure.

The radioactive damage or effects to the model must be slight enough so that these associated effects do not mask or override the aerodynamic effects which are being investigated.

These nuclear effects on the model are investigated to determine their influence on the design of the over-all system, and to determine if containment, greater than that implied by the thermodynamic limit of ten percent uranium, is required.

Chamber pressure and temperature are set at 1000 atmospheres and 10,000°K. A portion of the heat load to the moderator is absorbed by the flow of nitrogen entering the core, the remainder is removed by an external water flow enroute to another system component, the water diffusor. A seeded layer of carbon is used to provide a radiation barrier which protects the moderator from radiation heat loads.

The thermal energy of the hot gas in the reactor core is converted to kinetic energy in a convergent-divergent nozzle. The nozzle is cooled by conventional backside cooling and transpiration cooling, both utilizing a secondary flow of high pressure, but low enthalpy nitrogen.

A schematic of the test facility is given in Figure 3. A temperature - enthalpy diagram of the nitrogen cycle is given in Figure 4.

After the test section, the secondary nitrogen flow is vented into the main flow, reducing the temperature slightly. The stagnation temperatures are still in the vicinity of 10,000°K and prevent the use of conventional turbo-expansion devices or heat exchangers at this point.

A water spray diffusor is utilized to slow the flow and lower the stagnation pressure and temperature of flow to 1000°K and 100 atmospheres. The water spray is sufficient to cool the walls of the diffusor.

A centrifugal separator is used to separate the condensed uranium particles from the flow of superheated steam and nitrogen leaving the water diffusor.

At this point the flow is basically free of uranium and at a temperature and pressure at which conventional turbo-machinery can be employed. The flow has 2,500 megawatts of available power, if expanded only to the saturation point of the water. After this energy is removed from the stream, the water is condensed and separated. The nitrogen, at 0.24 atmospheres and 370°K,is cooled further in a conventional heat exchanger and pumped back to 1000 atmospheres using two multistage centrifugal flow compressors with interpump cooling to maintain temperatures below 1000°K. The power required for the pump work, 880 megawatts, is provided by the aforementioned turbine.

The pressure of the water is raised to 120 atmospheres in another multistage centrifugal pump, requiring 10 megawatts of the above turbine work.

The temperature - enthalpy diagram of the water cycle is given in Figure 5.

2.3 Component Interface Problems

To be successful as a system, the components of the facility must be mutually compatible. In the following sections, the operating characteristics of the reactor and the nozzle, which are the main components of the system, are examined. The reactor is examined to determine the effects of various operating pressures and fuel-nitrogen concentration on the critical size and fuel concentration.

Contamination of the model is examined to determine if it imposes a constraint on the fuel-nitrogen mixture in the core.

Heat transfer in the reactor and nozzle are also examined to determine limits on operating temperature, power and component size.

CHAPTER III

GASEOUS CORE NEUTRONICS

3.1 General

Reference 6 shows that the gaseous core nuclear reactor is theoretically feasible. It shows that one can obtain a reasonable estimate of reactor critical radius and critical fuel concentration by considering the reactor core to be a homogeneous mixture of fuel and moderator or a reflected sphere of fuel alone. The effects of containing the fuel with a gaseous annulus of hydrogen are also investigated as were the effects of multiple cavities. Reference 6 quantitatively shows that a gaseous core reactor can be designed with either simple or multiple cavity geometry.

In this study, the reactor will be considered to be a homogeneous mixture of pure uranium 235 and N_2 with a bare spherical geometry. The effects of reflecting the above bare sphere are also considered. One group neutron theory is utilized, that is, the neutrons are considered to be in thermal equilibrium with the reflector-moderator.

No attempt is made to separate the fuel from the working fluid, nitrogen. Criticality calculations

are made with the ratio of number density of nitrogen atoms to number density of fuel atoms, N_N/N_U, as a parameter. This gives one measure of contamination of the flow in the model test section. From the fluid dynamic point of view, the flow is treated as behaving as pure nitrogen, and the number density ratio gives a measure of how valid this approximation is. The model is also subjected to radioactive contamination, the number density ratio gives a partial measure of this effect; partial in that the uranium itself in the flow is not the only source of model contamination.

3.2 Criticality Condition

As a first approximation, the reactor can be considered to be a bare homogenous mixture of pure uranium 235 and nitrogen. Criticality is determined by considering all of the neutrons in the core to be thermal, that is, there is no loss of neutrons in the process of slowing down from the high energy state of production in the fission process, to capture at a lower thermal energy state. For steady state operation, the conservation of neutrons requires that the rate of production of neutrons in a control volume be equal to the rate of loss of neutrons due to absorption and leakage from the volume.

The rate of production of neutrons per unit volume is given by

$$\text{Production} = \nu \phi \Sigma_f \qquad 3.1$$

where ν is the average number of neutrons produced per thermal fission

ϕ is the neutron flux

and Σ_f is the macroscopic fission cross section of the core material.

The neutron leakage is given by the diffusion approximation as

$$\text{Leakage} = -D\nabla^2\phi \qquad (3.2)$$

where ∇^2 is the La Placian operator

and D is the diffusion coefficient, 1/3 of the transport mean free path in the reactor

The absorption term is similar to the fission term,

$$\text{Absorption} = \phi(\Sigma_a + \Sigma_f) \qquad (3.3)$$

here Σ_a is the macroscopic absorption cross section in the core.

Equations 3.1, 3.2 and 3.3 are combined and the conservation of neutrons is expressed in differential form by

$$D\nabla^2\phi + (\nu\Sigma_f - \Sigma_a)\phi = 0 \qquad (3.4)$$

or if the material buckling, B_M, is defined as

$$B_M^2 = \nu(\Sigma_f - \Sigma_a)/D \qquad (3.5)$$

the conservation of neutrons becomes

$$\nabla^2 \phi + B^2 \phi = 0 \tag{3.6}$$

For a spherical reactor, with the boundary conditions that the flux goes to zero at the radius of the core and the gradient of the flux is zero at the center of the sphere, Equation 3.6 can be solved for the geometric buckling of the reactor,

$$B_g^2 = \left(\frac{\pi}{R}\right)^2 \tag{3.7}$$

The criticality condition is the matching of the geometric buckling which satisfies Equation 3.6 with the material buckling of Equation 3.5. The diffusion length is defined as

$$L^2 = D/\Sigma_a \tag{3.8}$$

and the infinite multiplication factor as

$$k_\infty = \nu \frac{\Sigma_f}{\Sigma_a} \tag{3.9}$$

With this notation, the criticality requirement is

$$(\pi/R)^2 = \frac{k_\infty - 1}{L^2} \tag{3.10}$$

The criticality requirement for the system is that the geometric buckling be equal to the material buckling. This means that the rate of neutron creation due to fissions is equal to the rate of destruction of neutrons due to absorption, that is, fission and nonfission capture, and leakage from the critical region.

For a nitrogen and pure uranium 235 system, the number of neutrons released per thermal fission of uranium 235 is [18]

$$\nu = 2.46 \ \frac{\text{neutrons}}{\text{fission } U_{235}}$$

The interaction cross sections per atom for uranium, sub-subscript u , and nitrogen, sub-subscript N , are [18]

σ_{fu} = 580 barns
σ_{au} = 680 barns
σ_{aN} =1.88 barns
σ_{su} = 10 barns
σ_{sN} = 10 barns

where the subscripts f denotes fission,
a denotes absorption,
s denotes scatter.

With these cross sections, the criticality equation can be used to determine the number density ratio of nitrogen atoms to uranium atoms required for criticality as a function of the core radius and the number density of uranium 235 atoms,

$$\frac{N_N}{N_u} = 199 \pm \sqrt{4\times10^4 - \frac{1.845\times10^{47}}{R^2 N_u^2}} \qquad (3.11)$$

Using this relation the critical radius is found as a function of uranium 235 concentration with N_N / N_U as a parameter. The results are given in Figure 6 with the mass flow ratio of nitrogen to uranium shown in lieu of the number density ratio.

Examination of the criticality equation above shows

that as N_N/N_U decreases below 199, R_N must increase. Therefore, N_N/N_U = 199 gives the minimum reactor size for a given concentration, and the associated mass flow ratio is 15.4. This is due to the scattering contributions of the nitrogen atoms in the core reducing the transport mean free path of the neutrons. This is most readily seen if the criticality condition is expressed by

$$R^2 = \frac{\pi^2 \, 3(1-\cos\bar{\theta})}{N_U^2 \left(\nu \sigma_{fu} - \sigma_{au} - \frac{N_N}{N_U}\sigma_{au}\right)\left(\sigma_{su} + N_N/N_U \ \sigma_{su}\right)} \qquad (3.12)$$

where the macroscopic cross sections are replaced by the number density times the microscopic cross section. The denominator has a maximum value when N_N/N_U is 199. For higher or lower number density ratios, the critical radius increases.

As used here R is not the actual radius of the homogenous sphere, but rather that radius plus the extrapolation distance. The extrapolation distance is the distance at which the neutron flux, which has a finite value at the physical boundary of the sphere, goes to zero. Reference 9 gives the extrapolation distance as

$$\delta = 2.13\,D \qquad (3.13)$$

The physical radius of the bare sphere is

$$r = R - 2.13\,D \qquad (3.14)$$

This critical size and uranium concentration so obtained is only an approximation and is valid only in determining the effect of nitrogen poisoning of the reactor on critical size and critical uranium concentration. The actual reactor will be operating at elevated temperatures

which will effect the interaction cross section,which generally vary inversely with neutron energy. A higher equilibruim temperature means higher neutron energies and, in general, lower interaction cross sections. Also the actual reactor will not be bare but must be enclosed in some way.

The reactor core is in fact contained in a pressure vessel,for structural reasons the walls of which must be maintained at a low temperature relative to the reactor core. Lining the pressure vessel with beryllium, a moderator, which must also be cooled for structural reasons, provides a means of decreasing leakage from the core and a means of providing low energy neutrons to the core.

Nitrogen, being heavier than beryllium, does not absorb as much of the neutrons energy in a collision, therefore more nitrogen collisions are necessary to thermalize a neutron. Also nitrogen, even at very high pressures, is still very much less dense than the solid beryllium moderator and at the higher core temperatures, the scattering cross section for nitrogen is less than that for the cold beryllium moderator. It is reasonable to assume then, that the neutrons are in thermal equilibruim with the cool reflector and not with the hotter nitrogen-uranium mixture.

The effects of the reflector-moderator on core radius can be found from a one velocity, two region consideration. As before in the core, the conservation of neutrons is given by Equation 3.6.

In the reflector, there is no fissionable material and the conservation of neutrons gives

$$D_r \nabla^2 \phi_r - \Sigma_{a_r} \phi_r = 0 \tag{3.15}$$

where subscripts r and c stand for reflector and core respectively.

With the inverse of the square of the reflector diffusion length, L_r, defined as

$$K_r^2 = \Sigma_{a_r} / D_r \tag{3.16}$$

the neutron conservation equations in the core and reflector is obtained by dividing Equation 3.15 by D_r,

$$\nabla^2 \phi_c + B_c^2 \phi_c = 0 \tag{3.17}$$

and

$$\nabla^2 \phi_r - k_r \phi_r = 0 \tag{3.18}$$

This set of differential equations can be solved for a criticality condition with the boundary conditions

$$0 < \phi_c(r=0) < \infty \tag{3.19a}$$

$$\phi_c(r=R_r) = \phi_r(r=R_r) \tag{3.19b}$$

$$D_c \nabla \phi_c \Big|_{r=R_r} = D_r \nabla \phi_r \Big|_{r=R_r} \tag{3.19c}$$

and

$$\phi_r(R_r + d_r + \delta) = 0 \tag{3.19d}$$

where d_r is the reflector thickness
and R_r is the critical radius of the reflected core.

The solution of Equation 3.17 and 3.18 with boundary conditions of 3.19 gives an expression for the criticality of a reflected spherical reactor in the transcendental form,

$$D_r\left(k_r R_r \coth k_r(d_r + \delta) + 1\right) = D_c\left(1 - R_r B_c \cot B_c R_r\right) \qquad (3.20)$$

The reflected core radius can be expressed in terms of the bare core radius, r, and the reflector saving, S, as

$$R_r = r - S \qquad (3.21)$$

This value is substituted into Equation 3.20 and a transcendental expression for reflector saving is obtained,

$$\cot \frac{\pi S}{r} = \frac{D_r r}{D_s \pi} k_r \coth(d_r + \delta) - \frac{\left(1 - \frac{D_r}{D_c}\right)}{r - S} \qquad (3.22)$$

Equation 3.22 is solved graphically for the reflector saving at each known r, then the reflected core radius, R_r, is obtained by Equation 3.21

The resulting critical radii are plotted in Figure 7 against critical uranium concentrations for a 100cm beryllium reflector. Shown is the reflected core radius, with the mass flow ratio of nitrogen to uranium as a free parameter. Also shown are lines of constant pressure for

an operating temperature of 10,000°K.

Heat transfer in the reactor core, coupled with practical limits on the capacities of the system's pumps and turbines, lead to the choice of a minimum core radius.

Structural consideration dictates a low operating pressure, but this is not compatible with the desire to simulate the high stagnation pressures of a re-entry. Also, the problems associated with heat transfer in the core require high mass flows and low temperatures. For these reasons the operating pressure is set at the maximum possible with projected structural technology, that is, 1000 atmospheres.

While it is also desired that the mass flow rate of nitrogen to uranium be maximized so that the test facility simulate atmospheric conditions, the requirements for a minimum core size dominate in this case. It is also noted that the critical core radius increases rapidly with a slight increase in mass flow ratio from the minimum of 15.4

For these reasons the core radius is set at the minimum possible with a pressure limit of 1000 atmospheres. This radius is 170 centimeters, occuring at the mass flow ratio of 15.4

CHAPTER IV

MODEL NUCLEAR CONTAMINATION

4.1 Radiation Damage

In the gaseous core nuclear reactor used as a power source for this system, there is no provision made in the core itself for the separation of fuel and fission fragments from the working fluid. This makes the design of the reactor much more simple then if some hydrodynamic means of separation of fuel from the working fluid is utilized. As the system is closed there is no problem of venting radioactive material to the atmosphere ,relieving one of the major constraints that faces the use of a gas core nuclear rocket.

The presence of radioactive material in the fluid stream causes contamination of the model being tested. This contamination is examined to determine if the structural damage to the model will signicantly influence or mask the aerodynamic and thermal effects being tested. As the model must be examined after the test, the extent of radioactive contamination as a biological hazard also is examined.

Radiation damage is caused by neutron bombardment and interaction, alpha and beta bombardment and gamma radiation.[20]

The radiations may be divided into two groups. The light group consisting of betas, gammas and other electromagnetic radiations, and the heavy consisting of neutrons, fission fragments, accelerated ions, and alphas. As a general rule the damage from the heavy particles is more severe that that from the light particles.[20] The heavy particles displace the atoms of a solid crystal lattice from their normal position. In general this will result in an increased ultimate strength, a decrease in elongation and a reduction in area of the material, also the microhardness of the material increases and there is a decrease in impact strength. These effects are minimized if the neutron bombardment occurs at elevated temperature, as is the case in this test facility.

Graphite, a prime candidate for a re-entry material, incurs crystallite damage during irradiation. Hardness and strength are increased while thermal and electrical conductivities decrease. Graphite shapes change in gross dimension during radiation. All of these effects decrease in magnitude when the temperature of the graphite during radiation is increased, with almost no effect when graphite temperatures are above 1000°C. Also the integrated flux levels at which these effects begin to be noticable is high, of the order of 10^{19} neutrons per square centimeter.[20] As this test facility will provide very high model temperatures and neutron fluxes at the model of the order of 10^{15} neutrons/ cm^2 sec, it is expected that irradiation damage will have negligible effect on the test results.

4.2 Biological Hazards

In determining the biological radiation hazard due to model contamination the following assumptions are made:

i. radioactive particles, such as, fuel, fission fragments do not adhere to the model upon impact,

ii. contamination is due to neutron-model interaction causing a transmutation to a possibly unstable isotope,

iii. contamination is acceptable if the model can be handled with minimum protection within a short time of the test run,

iv. acceptable radiation levels from the model are 7.5×10^{-3} rem/hour as recommended by the US National Committee on Radiation Protection.[21]

4.2a Contamination Environment

Neutron density at the model has three sources; direct streaming from the reactor core, neutron flux from the fissionable mass in the test section, and secondary emission from fission fragments.

Direct streaming of neutrons from the core can be measured by noting the attenuation of the neutron flux by the gases in the nozzle between the model and the core.

The differential change in neutron flux due to absorption by the gas is

$$\frac{d\phi}{dx} = \phi \Sigma_a \qquad (4.1)$$

The macroscopic absorption cross section of the gas varies with position in the nozzle as the density of the gas decreases. Assuming this variation is linear with axial nozzle position, x , and that the density goes to zero at the model, Equation 4.1 becomes

$$\frac{d\phi}{dx} = \phi \Sigma_{a_o} \left(1 - \frac{x}{L}\right) dx \qquad (4.2)$$

When integrated and evaluated at the model, the flux at the model is given by

$$\phi_s - \phi_o e^{-L/2\lambda_{ao}} \qquad (4.3)$$

where L is the axial position of the model and λ_a is the absorption mean free path

The axial position of the model, L ,is limited by heat transfer considerations in the nozzle and inlet and must be minimized. Then L is the order of the required nozzle length to expand the flow to Mach 3, approximately 30 cm, for the throat size set in Section 6.1.

For the chamber condition of this study the mean free path for absorption in the chamber is about five times this value, then the free streaming flux from the core to the model is approximated by

$$\phi_s = 0.9\, \phi_o \qquad (4.4)$$

The neutron flux from the mass of fissionable material in the test section is found by considering the change in flux as the flow goes from the critical region of the core to the subcritical test section.

The time of flight from the core to the test section is of the order of the length divided by the speed of sound at the nozzle throat,

$$t_f = L/c^* \tag{4.5}$$

If the test section is considered to behave as an infinite cylinder with constant cross section, the critical buckling is a function of the geometry and is related to the test section radius by[9]

$$B^2 = \left(\frac{2.405}{R_t}\right)^2 \tag{4.6}$$

The effective multiplication factor in the test region is

$$k_{eff} = \frac{k_\infty}{1 + \left(\frac{2.405}{R_t}\right)^2 \frac{D}{\Sigma_a}} \tag{4.7}$$

where k_∞ is defined by Equation 3.9

With the assumption that the number of neutron generations is given by the time of flight, t_f, divided by the average neutron lifetime, $\bar{\lambda}_a/\bar{v}_n$, the neutron flux at the model, due to the reactivity of the fissionable gas in the test section, is given by

$$\phi_{\delta K} = \phi_0 \, e^{-\frac{t_f (k_{eff}-1)\bar{v}_n}{\bar{\lambda}_a k_{eff}}} \tag{4.8}$$

Equations 4.5 through 4.3 are evaluated for the conditions in this facility,

$$t_f = 5 \times 10^{-4} \text{ seconds}$$

$$k_{eff} = .002$$

$$\frac{k_{eff} - 1}{k_{eff}} = -500$$

to obtain the flux at the model due to the reactivity of the test section,

$$\phi_{\delta K} = \phi_o e^{-150} \tag{4.9}$$

As $\phi_{\delta K}$ is very much smaller than ϕ_s, it is considered negligible in this analysis.

Secondary emission of neutrons by fission fragments in the vicinity of the model will also contribute to the neutrons bombardment of the model. Given a fission fragment, A, with a half life, $t_{1/2 A}$, and a yield fraction per fission of η_A, from the definition of half life, the radioactive decay constant, λ, is

$$\lambda_A = \frac{\ln 2}{t_{1/2 A}} \tag{4.10}$$

The rate of creation of atoms of fragment A is

$$\frac{dA}{dt} = \eta_A \Sigma_f \phi_o \tag{4.11}$$

where $\Sigma_f \phi_o$ is the number of fissions per unit volume per unit time.

The rate of decay is

$$\frac{dA}{dt} = -\lambda_A A \tag{4.12}$$

Thus in the reactor, fission products, A, build up at the rate

$$\frac{dA}{dt} = \eta_A \Sigma'_f \phi_o - \lambda_A A \tag{4.13}$$

and concentration of species A at time t is

$$A(t) = \frac{1}{\lambda_A}\left(\eta_A \Sigma_f \phi_0 - \left\{\eta_A \Sigma_f \phi_0 - \lambda_A A_0\right\} e^{-\lambda_A t}\right) \tag{4.14}$$

With the initial condition that the initial concentration of species A is zero, the concentration of fragments leaving the core is given by $A(t_o)$, where t_o is the dwell time of fluid in the core,

$$t_D = \frac{\rho_0 V_{OLC}}{m} \tag{4.15}$$

At $t_D = 1\,\text{second}$, the concentration of A leaving the reactor is given by

$$A(1) = \frac{\eta_A \Sigma_f \phi_0}{\lambda_A}\left(1 - e^{-\lambda_A}\right) \tag{4.16}$$

The rate of decay in the nozzle is given by Equation 4.12 evaluating this at the test section with a time of flight, t_f, from the core, the rate of decay of fragment A at the model is

$$\frac{dA}{dt} = -\lambda_A \frac{\eta_A \Sigma_f \phi_0}{\lambda_A}\left(1 - e^{-\lambda_A}\right) e^{-\lambda_A t_f} \tag{4.17}$$

If it is assumed that one neutron is emitted per decay, the sum over all fission fragments of the decay rates given by Equation 4.17 is the rate of creation of neutrons at the model,

$$\frac{dn}{dt} = \sum_A \eta_A e^{-\lambda_A t_f}\left(1 - e^{-\lambda_A}\right) \Sigma_f \phi_0 \tag{4.18}$$

The absorption mean free path in the test section is about fifty times larger than the test section radius, therefore all neutrons freed in the test section will hit the model or walls. If all neutrons hitting the walls are absorbed, the ratio of neutrons hitting model to those

hitting the wall is given by the ratio of model radius to test section radius, R_m / R_t. For negligible model blockage of the test section assume this ratio is 0.1

Then the delayed neutrons strike a unit area of the model at a rate

$$\phi_d = \frac{A_t}{2\pi R_m} \frac{R_m}{R_t} \frac{dn}{dt} \qquad (4.19)$$

The fission products yield are given in Reference 22.

An examination of the distribution of fission products shows that for a mass number less than 80 or greater than 160, η_A is less than one part in ten thousand and the contribution to ϕ_d is negligible regardless of the half life. Also, if $t_{1/2}$ is greater than one minute, λ_A is less than .01 seconds^{-1}, this combined with a maximum η_A of ten percent from Reference 22, shows that the contribution of any element with a half life much greater than one minute may be ignored in approximating the neutron flux due to secondary emission from fission fragments. References 20 and 22 were examined for fission products with yield fractions greater than 10^{-4} and half lives less than one minute. The isotopes satisfying these criteria are given in Table 1. With these values, the rate of creation of neutrons at the model is, by Equation 4.18, 1.72×10^{-2} neutrons per second and the neutron flux at the model due to secondary emission of neutrons is

$$\phi_d = 2.3 \times 10^{-4} \phi_o \qquad (4.20)$$

It is noted that this method gives a conservatively high estimate of flux at the model due to assuming that

the total fission yield for a given atomic number indicated in Reference 23 is the element with the atomic number with a short half-life, and further that these radionuclides all emit a thermal neutron upon decay.

There are two unconservative assumptions in this development, that is that the initial condition is the absence of fission fragments at the beginning of the reactor dwell time, and that only short lived neutron emitters are involved. In operating as a closed cycle, the supply of nitrogen and uranium will be contaminated by the fission fragments generated during previous residence in the reactor core, increasing the initial concentration of fragments and allowing build up of fission fragments with a long half-life.

Due to the shear magnitude of the power involved in this facility, it is expected that the time for a given mass of fluid to complete a cycle will be long enough to allow decay in the concentration of the prompt neutron emitters and that provision can be made for monitoring and removal of long lifed fission fragments as a part of the fuel handling process.

With these assumptions, the flux due to secondary emission from fission fragments is several orders of magnitude smaller than the direct streaming flux, and the former is neglected.

The flux striking the model is then approximated by the direct streaming neutron flux of Equation 4.4 .

The average flux in the gaseous core is set by the reactor size, the power required, the energy per fission, ϵ, and the macroscopic cross section for fission of the fuel in the reactor core,

$$\phi_0 = \frac{P/V_{ol}}{\Sigma_f \epsilon} \tag{4.21}$$

At a power level of 7100 megawatts with a 1.7 m core, the average flux in the gas core is 3.26×10^{15} neutron/cm^2 sec.

Equation 4.4 gives the flux at the model for these conditions, 2.93×10^{15} neutrons/ cm^2 sec.

4.2b Model Contamination

The radiation hazard from the model is assumed to consist of secondary emission from neutron flux induced radionuclides on the model. The governing equation is of the same form as the build up of radionuclides in the core, then decaying after exposure. The build up of species A on the model during a test run of time, t_T , is

$$A(t_T) = \frac{\Sigma_{B,A}}{\lambda_A} \phi_m \left(1 - e^{-\lambda_A t_T}\right) \tag{4.22}$$

where $\Sigma_{B,A}$ is the neutron macroscopic absorption cross section in the reaction $B + {}_0n^1 \rightarrow A$ and B is one of the original materials of the model or a transmuted species. The rate of decay of A after the test is

$$\frac{dA}{dt} = \Sigma_{BA} \phi_m \left(1 - e^{-\lambda_A t_T}\right) e^{-\lambda_A t} \tag{4.23}$$

where t is the time since exposure to the neutron. After the decay rate for a species has been determined, the type

of decay must be examined to determine the mode of decay, that is alpha, beta, gamma or neutron emission and the energy of the emitted particle.[22] The particle type and energy set the maximum decay rate that a man can be exposed to and not exceed the limits of .006 rem/day. It is noted that if more than one species is formed or more than one mode of decay is present, the sum of the exposures will determine the allowable decay rates of each species or mode.

As graphite is the prime candidate for material to be tested, it will be examined. Carbon undergoes the reactions

$${}_6C^{12} + {}_0n^1 = {}_6C^{13} \quad \text{stable} \qquad (4.24a)$$

$${}_6C^{13} + {}_0n^1 = {}_6C^{14} \quad t_{1/2} = 5570 \text{ years} \qquad (4.24b)$$

$${}_6C^{14} + {}_0n^1 = \beta^- + {}_7N^{14} \quad \text{stable} \qquad (4.24c)$$

for

$N_{c_{12}} = 8.55 \times 10^{22}$ atom/cm^3

$\sigma_{c_{12},c_{13}} = 3.3 \times 10^{-27}$ cm^2

$\sigma_{c_{13},c_{14}} = .9 \times 10^{-27}$ cm^2

$t_T = 200$ seconds

$$\Sigma_{c_{12},c_{14}} = (N_{c_{12}} \sigma_{c_{12},c_{13}} \phi_m t)(\sigma_{c_{13},c_{14}}) \qquad (4.25)$$

The initial decay rate for the model is, by Equation 4.23

$$\frac{dC_{14}}{dt} = 8.4 \times 10^{-7} \; \frac{(.15\,\text{Mev})\beta}{\text{cm}^3\ \text{sec}}$$

With no absorption in the model, the surface beta flux for a cylinderical model is conservatively given by

$$\frac{dC_{14}}{dt}\,\frac{Vol_M}{A_M} \cong \frac{dC_{14}}{dt}\,\frac{R_M}{2} \qquad (4.26)$$

For a carbon model with a radius of 1.25 centimeters

$$\frac{dC_{14}}{dt} = 5.27 \times 10^{-7} \; \frac{(.15\,\text{Mev})\beta}{\text{cm}^2\ \text{sec}}$$

Reference 20 gives the exposure of betas of various energies which produces an allowable dose of .006 roentegen equivalent man per eight hour day. The exposure rate above is on the safe side, therefore a graphite model may be handled immediately after a run at 7,100 Megawatts for 200 seconds.

Correlations between nuclear decay products and allowable dose rates are readily available in the literature[9,20,23]. A very slight protective layer, such as paper or cloth, will provide protection against alpha particles, which do not present an external radiation hazard.[9,20]

It is also probable that high percentages of hydrogen[2] will be present in an ablative material, and the decay of hydrogen isotopes yields a low energy beta particle in concentrations, determined by Equation 4.22, five orders of magnitude below carbon and therefore, as a graphite model, also may be handled immediately after a test.

This analysis can not possibly determine if each and every material will be safe to handle after a test. The user will have to examine the reaction of each model individually to determine the contamination from each material and the time history of resulting total model contamination, as given by Equation 4.22 summed over all model components. The resulting model activity can be compared to allowable dose rates to determine if and when the model can be handled.

It is noted by examination of Equations 4.4, and 4.22 that the decay rate at the model is directly proportional to the flux rate in the reactor. This in turn, by Equation 4.20,

is dependent on the specific power of the reactor and varies inversely with the concentration of uranium in the core, so that low power density and high uranium concentration are desired.

As is shown in Section 6.1, the operating power of the reactor is proportional to the area of the core, with core temperature and pressure fixed. The specific power varies then inversely as the core radius, as does the concentration of uranium in the core at small radii, shown in Figure 7.

It can be concluded that, at least, for many possible re-entry materials there would be no difficulty in handling the models after testing and that model contamination is not a critical parameter in the design of this system, but should a particular material to be tested become highly contaminated, the degree of contamination can be reduced by reducing either the test duration or the specific power density. It is assumed that this does not occur in this study.

CHAPTER V

REACTOR COOLING

5.1 Heat Loads

The walls of the gaseous core reactor are subjected to high heat loads due to convective, conductive and radiation heat transfer and heat producing nuclear reactions in the solid materials of the core materials.

At the high temperatures of the core the heat load due to radiation transfer is much greater than the convective and conductive heat loads: the convective and conductive heat loads are considered negligible in this analysis. The core is assumed to radiate as a black body at 10,000°K and the walls absorptivity set as 0.6.

The heat load due to nuclear reactions is assumed to be due to neutron and gamma fluxes from the core and is set as eight percent of the power output[9] divided by the core area.

The heat load per unit wall area is

$$Q_{oc} = \epsilon \sigma T_o^4 + .08 \, P/A_c \qquad (5.1)$$

where

ϵ is the wall absorptivity, and
σ is the Stephan-Boltzmann constant

For the conditions of this study, the heat load to the wall, given by Equation 5.1 is

$$Q_{oc} = 8.48 \times 10^3 \ \text{cal/cm}^2\text{-sec.}$$

5.2 Criticality Effects

The loads given by Equation 5.1 are much too high for the thick beryllium moderator to conduct away from the core, and are predominantly due to radiation. Reference 7 suggests the use of a thermal barrier, cooled by transpiration and radiation seeding to protect the walls of a gaseous core nuclear rocket under similar high radiation heat loads. This method of cooling is not appropriate for use in the reactor used in this system. The large size of the reactor is due to the high absorption cross section of the working gas, nitrogen. This causes a low value of the infinite multiplication factor in the reactor, K_∞, given by Equation 3.9. Examination of Equation 3.9 shows that increasing the macroscopic absorption cross section in the core will reduce the infinite multiplication factor, K_∞. As this is already very close to 1.0 in this reactor, addition of even a small thermal barrier causes the reactor to be subcritical for any reactor size.

Even if a material, with sufficiently low neutron absorption characteristics and high strength could be found, the transpiration flow necessary to internally cool the thermal barrier is not available due to the large area of this core and the relatively small throat area.

The moderator in this study is protected from the high thermal radiation heat loads by a seeded layer of carbon particles in the core near the walls. The small amount of carbon necessary to protect the walls does not preceptibly lower the multiplication factor, but has a more pronounced effect on lowering the diffusion length, defined by Equation 3.8 , so that the carbon acts as a moderator and slightly decreases the critical size, as shown by Equation 3.10 . This effect is due to the very small absorption cross section of carbon, which effects k_∞, and the larger scattering cross section, which reduces L . The effect of the carbon seed on criticality is ignored in this analysis.

5.3 Reactor Flow Pattern

In order to protect the moderator of the core, it is necessary to establish the following flow pattern. Consider any diagonal plane which includes the axis of symmetry of the nozzle. The reactor core flow and the nozzle are axisymmetric. The reference direction, $\theta = 0$, is aligned with the nozzle axis; the flow has a source at $\theta = \pi$, the fuel and nitrogen inlet, and a sink at the nozzle. A boundary layer is formed along the walls as the flow proceeds from inlet to the nozzle, much like a low speed divergent-convergent nozzle.

The uranium fuel, in the form of a fine powder mixed with nitrogen, is sprayed into the core at the $\theta = \pi$ position. The nitrogen is sprayed into the core through a annulus around the fuel nozzle. Perfect mixing of the fuel and nitrogen is assumed. It is assumed that the carbon seed tends to remain toward the walls and is limited to a layer

one-tenth of the core radius thick and starting at the core wall.

The gamma and neutron fluxes to the moderator is unaffected by the thermal radiation barrier. The total heat load to the moderator is the sum of the nuclear heat load and the thermal radiation which is not absorbed by the seeded layer. The moderator is cooled by a combination of radial injection of a fraction of nitrogen flow into the core, and water cooling. The nitrogen flow itself is not sufficient to cool the moderator and must also be used to establish the desired flow pattern.

5.4 Radiation Barrier

With the flow pattern in the core as established in paragraph 5.3, the flow is essentially flow in a nozzle with a diverging section proceeding the converging-diverging nozzle. Reference 12 gives the results of using a seeded layer to protect a gaseous core rocket nozzle. With perfect mixing of the fuel and working fluid, a seeded layer 1/10 of the local nozzle radius thick will reduce the radiant energy flux by two orders of magnitude if the seeded layer absorption coefficient, κ , is 1/3 centimeter^{-1}.

Reference 13 gives a correlation of the total absorption coefficient per seed particle concentration, κ / N, and the particle radius. Using carbon particles as the seeding material, it is desired that the average concentration of carbon particles be minimized, both for nuclear and thermodynamic reasons.

The average carbon density, $\bar{\rho}$, in the seeded layer is

$$\bar{\rho} = \frac{K}{K/N}\left(\rho_s \frac{4\pi}{3} R_s^3\right) \qquad (5.2)$$

where

ρ_s is the mass density of the carbon seed

and R_s is the average seed radius

With K set at $\frac{1}{3}$ cm^{-1}, the average density is minimized at 3.7×10^{-7} gram/centimeter^3 ; this occurs with a concentration of 4.5×10^{10} particles/cm^3 having an average diameter of 0.1 microns.

As the seeded layer does not fill the core, the average seed density over the core is

$$\bar{\rho}_c = \frac{\bar{\rho}\,\frac{4}{3}\pi\left(R_c^3 - .9R_c^3\right)}{\frac{4}{3}\pi R_c^3} \qquad (5.3)$$

$$= 1 \times 10^{-7} \text{ grams/centimeter}^3$$

The contribution to the macroscopic absorption cross section due to the carbon atoms in the core is given by

$$\Sigma_{a_c} = \frac{\bar{\rho}_c \mathcal{A}}{\mathcal{M}_c}\sigma_{a_c} \qquad (5.4)$$

where $\mathcal{A}$ is Avogadros number and $\mathcal{M}_c$ is the molecular weight of carbon.

For the concentration of carbon in the core due to the seeded thermal barrier, Equation 5.4yields an absorption cross section contribution of 1.6×10^{-7} centimeter^{-1} . As this is four orders of magnitude less than the absorption

cross section of the nitrogen and uranium mixture in the core, the presence of the carbon seed on criticality is ignored.

5.5 Moderator Cooling

The seeded radiation barrier discussed in Section 5.4 reduces the radiant heat load to the wall, given in Section 5.1, by two orders of magnitude, but does not effect the nuclear radiation induced heat load. The resulting heat load to the moderator is 350 cal/cm^2 sec.

The thickness of the moderator and the thermal conductivity of beryllium prevent this heat load from being conducted through the moderator and removed by back side cooling.

A portion of the incoming nitrogen flow is radially passed through the moderator to absorb the heat load to the moderator. The coolant nitrogen flow is injected tangentially into the core in such a manner as to be parallel to the flow of the boundary layer at the point of injection. This is to prevent the injected flow from driving the seeded thermal barrier away from the wall. A small amount of carbon, as is necessary to replace carbon in the thermal barrier which vaporizes or diffuses out of the thermal barrier, is carried by the cooling nitrogen flow.

The maximum temperature of the beryllium moderator is set at 1000°K by structural strength limits.With one half of the primary nitrogen flow used to establish the desired flow pattern, the remaining primary nitrogen flow is capable of absorbing one third of heat load in the moderator, increasing

in temperature from 293 °K to 1000 °K. The remaining heat load is absorbed by bleeding four percent of the water flow enroute to the water diffusor and allowing its temperature to increase to 1000 °K in the moderator.

CHAPTER VI

NOZZLE HEAT TRANSFER

6.1 Nozzle Size

The hot gases in the core are radiating energy away from the core. As the moderator walls are not capable of transferring this heat load, they must be protected by a seeded thermal barrier, and the absorbed energy carried out of the core through the nozzle. Thus the minimum operating power is set by the radiant heat load from the core, and the size of the core wall surface. The nozzle throat area is found by equating the radiative power in the core to the energy flow through the nozzle, then,

$$A_* = \frac{Q_{oc} A_c}{\rho_* V_* H_o} \tag{6.1}$$

For the operating conditions set in Section 2.2, the minimum throat size is 93 centimeters^2.

6.2 Heat Loads

Large heat loads are experienced by the walls of the nozzle as the flow is accelerated from stagnation conditions of the core to the high Mach number desired in the test section. The heat load is due to convective and radiative heat transfer from the hot gases and nuclear heating of the nozzle walls by alpha, beta and gamma interaction. To

prevent failure of the nozzle, this heat load must be transferred through, absorbed by or blocked from the nozzle walls.

Turbulent flow is assumed in the nozzle, also it is assumed that the flow is frozen, isentropic and one dimensional in determining local flow properties. The heat generated in the nozzle by nuclear interaction is assumed negligible compared to the convective and radiation heat loads.

6.3. Nozzle Configuration

The nozzle consists of a series of longitudinal porous tubes, the area ratio of which is adjusted to provide an over pressure, of the cooling fluid in the nozzle tubes above the pressure of the flow in the nozzle, of 10 atmospheres. This provides the driving potential for transpiration cooling of the nozzle. Flow inside the coolant tubes is assumed to be turbulent.

The tube cross section is a "U" shape, the flat sides of which may vary to provide the desired area ratio and also to facilitate joining the tubes together to form a smooth nozzle shape. The heat transfer surface is approximated by a circle whose radius is R. The fin effect of the radial sides of the cooling tubes is not accounted for, giving a conservative value for the heat transfer to the coolant.

The coolant tubes support the thermal stress due to heat transfer across their radially inner-most face. They also support the hoop stress due to the coolant pressure. The tubes are closed by a shell which supports the pressure

of the hot gas in the nozzle.

6.4 Maximum Heat Transfer

The maximum heat load that can be transferred through the wall is set by the material properties, the configuration of the wall and the pressure the wall must support.

For a thin walled tube, with the wall thickness, d, very much less than the tube radius, R_t, the temperature gradient across the tube is linear. The thermal stress across the tube, in the tangential direction, are maximum in tension at the cool inner fiber,

$$\sigma_{th} = +\alpha E\Big|_{T_{w_o}} (T_w - T_{w_o})/2 \qquad (6.2a)$$

and maximum in compression at the hot outer fiber

$$\sigma_{th} = -\alpha E\Big|_{T_w} (T_w - T_{w_o})/2 \qquad (6.2b)$$

where

α is the coefficient of linear expansion,
E is the modulus of elasticity,
T_w is the hot side wall temperature,
T_{w_o} is the cold side wall temperature,

and both α and E are functions of temperature.

The pressure differential across the cooling tube wall, p, causes a uniform hoop stress in the wall,

$$\sigma_h = \pm \frac{p R_t}{d} \qquad (6.3)$$

where

d is the wall thickness,

and the positive sign indicates tensile hoop stress, the negative compressive.

The total stress is given by the sum of the thermal and hoop stress; scaler sum in this case as both are tangential.

At the extreme fibers,

$$\sigma = \pm \frac{\alpha E(T_w - T_{wo})}{2} + \frac{p R_t}{d} \tag{6.4}$$

The configuration chosen in this analysis utilizes a series of small cooling tubes forming the nozzle. This gives a tensile hoop stress and the maximum total stress is tensile at the cool inner fiber. The hoop stress relieves the compressive thermal stress at the hotter inner wall, where the material is weakest.

The heat transferred through the wall is given by,

$$Q = \frac{k}{d}(T_w - T_{wo}) \tag{6.5}$$

where

k is the wall thermal conductivity

Equation 6.4 is solved for the temperature across the wall, and this is substituted into Equation 6.5 ,

$$Q = \frac{\sigma - \frac{p R_t}{d}}{\frac{\alpha E \; d}{2k}} \tag{6.6}$$

The maximum heat transfer through the wall, with respect to wall thickness, d, is obtained by setting, dQ/dd equal zero

$$\frac{4kpR_t}{\alpha E d^3} - \frac{2\sigma k}{\alpha E d^2} = 0 \tag{6.7}$$

The condition for maximum heat transfer through the wall is,

$$\frac{\sigma_u}{2} = \frac{p R_t}{d} = \sigma_h = \sigma_{th} \tag{6.8}$$

The maximum heat flow through the wall is

$$Q_{max} = \frac{\sigma_u^2 k}{2 \alpha E p R_t} \tag{6.9}$$

Here failure occurs when the tensile stress at the inner fiber of the coolant tubes reaches the ultimate stress of the tube material. Radial stress is due to the pressure differential across the tube thickness and is negligible compared to the tangential stress. The nozzle has incroporated an expansion-slip joint at the up stream, low Mach end; this prevents longitudinal thermal stress so that the stress in the coolant tubes is considered uniaxial.

6.5 Material Selection

A material was sought with a maximum value of $\frac{\sigma_u^2 k}{\alpha E}$ in order to maximize heat transfer with respect to material selection. This parameter is a function of temperature in a given material and the temperature must be high enough so that super-cooling is not necessary at the back side to absorb the heat load. Wall temperature also affects the heat load to the wall but examination of the Bartz's Equation[10], utilized to determine the convective heat load, shows only a weak dependence of convective heat transfer on wall temperature.

This investigation chooses Rene 41[24] at T_w of $1025^{\circ}K$ as having the desired structural properties.

At this temperature,

σ_u is 146,000 pounds/inch^2

E is 2.4 x 10^7 pounds/inch^2

K is 0.05 cal/cm-sec-$^\circ$K

α 1.57 x 10^{-7} cm/cm$^\circ$K

Minimum wall thickness is set by manufacturing limitations and is assumed to be 0.01 cm for this analysis.

This choice of material and wall thickness gives a maximum heat transfer per unit wall area of

$$Q_{MAX} = 1.94 \times 10^3 \text{ cal/cm}^2 \text{ sec}$$

provided that the cooling tube radius, set by Equation 6.8 with a ten atmosphere pressure differential across the wall, is 5 cm or less. The temperature drop through the wall is

$$T_w - T_{w_0} = 389^\circ k$$

and $$T_{w_0} = 636^\circ k$$

6.6 Test Section Mach Number

The nozzle shape considered is a convergent-divergent nozzle formed by the previously defined cooling tubes. The nozzle is axially symmetric with a 45 degree convergent section, 15 degree divergent section and a radius of curvature at the throat equal to the throat inner radius.

The heat load to the nozzle is weakly dependent upon throat radius, affecting the convecting heat transfer coefficient only in this analysis. The pump work required of

the system as a whole, however, varies directly with the mass flow, which varies as the area of the throat.

The throat radius is chosen in Section 6.1 as 5.45 centimeters.

The test section Mach number is arbitrary with a frictionless isentropic nozzle. In this nozzle, transpiration cooling is required until the flow has expanded to about Mach 6, which requires a lengthy nozzle, of the order at 15 meters. Expanding the flow to Mach 6 increases the transpiration coolant requirement and nozzle losses. For this analysis, a test section Mach number of 3.0 is chosen to enable simulation of the desired flow fields, but reduce transpiration pumping requirements and nozzle losses.

6.7 Transpiration Cooling Requirements

The heat load per unit area to the wall, neglecting gamma heating, is given by,

$$Q = Q_{oc} + Q_r \tag{6.10}$$

where Q_{oc} is the convective heat load in the absence of transpiration cooling,

Q_r is the radiative heat load, assumed unaffected by transpiration cooling.

The convective heat load was obtained by the method of Bartz[10] for turbulent compressible flow,

$$Q_{oc} = h\,(T_{Aw} - T_w) \tag{6.11a}$$

where
$$h = \left[\frac{.026}{D_x^{.2}}\left(\frac{\mu^{.2} C_p}{P_r^{.6}}\right)_o \left(\frac{p_o\, g}{c_x}\right)^{.8} \left(\frac{D_*}{r_c}\right)^{.1}\right]\left(\frac{A_*}{A}\right)^{.9} \sigma \tag{6.11b}$$

$$\sigma = \frac{1}{\left[\frac{1}{2}\frac{T_w}{T_o}\left(1+\frac{\gamma-1}{2}M^2\right)+\frac{1}{2}\right]^{.8-\frac{\omega}{3}}\left[1+\frac{\gamma-1}{2}M^2\right]^{\frac{\omega}{5}}} \qquad (6.11c)$$

h is the heat transfer coefficient,

ω is 0.6,

D is the throat diameter, inches,

μ is the viscosity,

C_p is the specific heat at constant pressure,

T is the temperature, °R ,

sub$_w$ = wall,
sub$_o$ = bulk,
sub$_{aw}$ = adiabatic wall,

P_o is the chamber pressure,

r_c is the radius of curvature of throat, inches,

$\frac{D_*}{r_c}$ is 1 for the nozzle,

A_*/A is the nozzle area ratio,

γ is the ratio of specific heats,

M is the Mach number.

The thermodynamic properties of nitrogen[14] were used in this analysis, and the presence of the uranium was ignored.

The radiation heat load is obtained by considering the gas to radiate at stream ambient temperature as a black body and the wall to have an absorptivity of 0.6,

$$Q_R = \epsilon_w \sigma T_4 - \alpha_w \epsilon_w \sigma T_w^4 \qquad (6.12)$$

The radiation from the wall is negligible compared to the load to the wall and this reduces to

$$Q_R = \epsilon_w \sigma T^4 \qquad (6.13)$$

where

ϵ_w is the wall absorptivity,
ϵ_N is the gas absorptivity,
σ is the Stefan-Boltzmann constant,
T is the Temperature, ambient free stream °K,
α_w is the wall emissivity.

The heat load to the nozzle wall in the absence of transpiration cooling is given in Figure 8 . The maximum heat load that the wall is capable of withstanding is lower than the load experienced. Transpiration cooling by the injection of low temperature nitrogen is used to reduce the convective heat load to the wall.

The effects of transpiration cooling in reducing the convective component of heat transfer is given in Referencell. The results are given in terms of the Stanton number reduction obtained by injection of a homogeneous coolant into a turbulent nozzle flow verses a blowing parameter, F/S_{T_0}. Here F is defined as the ratio of the transpirant mass velocity to the local free stream mass velocity,

$$F = \frac{G}{\rho V} \tag{6.14}$$

where G is defined as the transpiration mass velocity. The Stanton number is defined as,

$$S_T = \frac{h}{\rho V c_p} \tag{6.15}$$

Then the Stanton number reduction is, to the first order, the reduction in convective heat load,

$$S_T / S_{T_0} = Q_c / Q_{c_0} \tag{6.16}$$

The maximum heat load transferred through the wall, with transpiration cooling, is the sum of the reduced convective heat load and the radiation heat load minus the heat absorbed by the coolant passing through the wall.

$$Q_{max} = Q_c + Q_R - G\bar{c}_p(T_w - T_{wo}) \qquad (6.17)$$

where $\bar{c}_p$ is evaluated at local pressure and the average temperature in the wall.

The convective heat load without transpiration cooling is given by,

$$Q_{co} = h_o(T_{Aw} - T_w) \qquad (6.18)$$

and

$$\frac{G\bar{c}_p}{h_o} = \frac{F}{S_{To}} \frac{\bar{c}_p}{c_p} \qquad (6.19)$$

With Equations 6.18 and 6.19 the maximum heat flow through the wall can be rearranged to

$$\frac{Q_{MAX}}{Q_{oc}} - \frac{Q_R}{Q_{oc}} = \frac{Q_c}{Q_{oc}} - \frac{F}{S_{To}} \frac{\bar{c}_p}{c_p} \frac{(T_w - T_{wo})}{(T_{Aw} - T_w)} \qquad (6.20)$$

The left hand side of this equation is known at each station and the right hand side suggests the possibility of a graphical solution using the difference between the Stanton number reduction data of Reference 11 and a family of straight lines of slope $\bar{c}_p(T_w - T_{wo})/c_p(T_{Aw} - T_w)$. Figure 9 reproduces the Stanton number reduction data of Reference 11 and illustrates the graphic method of solution. The blowing parameter, F, is obtained by this method and from it, the transpiration mass velocity necessary to reduce the heat

load through the wall to the maximum allowable. This flow is graphically integrated to obtain the total required transpiration flow.

The transpiration cooling flow per unit axial nozzle length, $2\pi RG$, is given in Figure 10, along with the total transpiration mass flow.

Under the conditions of this study, the transpiration coolant flow necessary to prevent thermal damage to the nozzle and test section is 1.25×10^5 gram/second, and the ratio of transpiration flow to the primary flow in the nozzle is,

$$\frac{m_{tr}}{m} = 0.37$$

This estimate on transpiration cooling requirement is conservatively high as the flow is assumed to radiate as a black body and the effects of thermal radiation blockage by the seeded layer in the core is neglected.

6.8 Secondary Nitrogen Flow

The heat flow through the wall must be absorbed by the flow in the coolant tubes. The flow properties in the tubes are set by matching the heat transfer at the throat as this is the point of maximum heating load.

The flow in the tubes can not be set point by point to enable maximum heat transfer to be possible along the entire length of the nozzle and heat transfer rates below Q_{max} are possible along the nozzle. This problem is recognized but not investigated further in this analysis as it is felt that the transpiration cooling flow can be

tailored[11] to fit a wall with variations in heat transfer capabilities.

The heat flow through the walls is absorbed by the coolant flow,

$$Q_{max} = h_c (T_w - T_c) \tag{6.21}$$

Here radiation and nuclear heating of the coolant are ignored. The coolant is flowing in a nozzle shaped duct but here fluid is bled out of the tube. In the absence of data on sucking of a turbulent boundary layer, the data of Reference 11 is extrapolated to include the sucking case. This is also illustrated in Figure 10, and is analogous to the treatment of a sucked laminar boundary layer given in Reference 25.

The method of Bartz is used as before to determine the heat transfer coefficient. The coolant tube nozzle throat radius is set at .5 cm.

The chamber temperature and pressure of the secondary nitrogen flow is set by matching the heat transfer through the wall at the throat to the heat absorbed by the coolant of that point, taking into account the effect of the transiration cooling flow sucking the boundary layer in the coolant tubes.

For the conditions of this study, the secondary nitrogen chamber pressure is 1010 atmospheres and the temperature is 530 °K. With these chamber conditions the mass flow of secondary nitrogen is 2.17×10^5 grams per second and the ratio of secondary to primary nitrogen flow is 0.67 to 1.

The secondary flow of nitrogen that is used to provide transpiration and backside cooling of the nozzle is approximately the same as the primary flow through the nozzle. This doubles the amount of pump work required, but as the nozzle would fail without the transpiration protection, this additional pump work is an acceptable penalty that must be incorporated into the design of the system.

CHAPTER VII

AUXILIARY EQUIPMENT

7.1 General

Operating this facility as a closed cycle removes some of the technological problems involved in the design of a gaseous core rocket. The problem of containing the gaseous fuel in the reactor core is avoided here by operating as a closed cycle. This introduces the problem of additional equipment in the cycle. Among the additional equipment needed are high powered turbines, high capacity pumps, large heat exchangers and fuel separation and processing equipment.

7.2 Water Diffusor

The flow at the exit of the test section is mixed with the secondary nitrogen flow which was utilized to provide transpiration and backside cooling of the nozzle. At this point the flow stagnation temperature, determined from the enthalpy of the mixture, is 8000°K and the stagnation pressure, assuming isentropic expansion through the nozzle, is 1000 atmospheres.Conventional heat exchangers can not operate at these temperatures and pressures, neither can conventional turbo-machinery. To lower the stream's temperature and pressure, a water spray diffuser is employed. The water is sprayed directly into the hot nitrogen stream and is heated to super-heated steam by the nitrogen, which loses energy in the process.

The cross sectional area of the diffuser can be designed to obtain the desired outlet conditions.

Conservation of energy determines the required water flow. Conservation of energy requires that

$$m_w H_w(T_{w_1}, P_{w_1}) + m_N H_N(T_{0_1}, P_{0_1}) = m_w H_w(T_{0_2}, \xi P_{0_2}) + m_N H_N(T_{0_2} \{1-\xi\} P_{0_2}) \tag{7.1}$$

where m is the mass flow rate
H is the total enthalpy
ξ is the mole fraction of water
$1-\xi$ is the mole fraction of nitrogen

and subscript w refers to water
1 inlet conditions
0 stagnation conditions
2 outlet conditions.

Equation 7.1 was utilized to obtain the required mass flow of water necessary to reduce the temperature and pressure of the nitrogen stream to the desired values.

The size of the water diffuser is set by the perfect gas law, written in the form

$$\frac{P_1}{P_2} = \frac{A_1}{A_2} \frac{m_2}{m_1} \frac{M_1}{M_2} \sqrt{\frac{T_2 \bar{\gamma}_1 \bar{\mathcal{M}}_1}{T_1 \bar{\gamma}_2 \bar{\mathcal{M}}_2}} \tag{7.2}$$

where all values are static values and
$\bar{\mathcal{M}}$ is the mixture average molecular weight
$\bar{\gamma}$ is the mixture average specific heat ratio

With the properties of nitrogen given in Reference

14 and those of water from Reference 26, Equations 7.1 and 7.2 can be used to find the necessary water flow and diffusor exit area, once the exit Mach number, temperature and pressure are specified.

The diffusor outlet total temperature is set at 1000°K, as an upper operating temperature for turbo-machinery. The outlet total pressure is set a 100 atmospheres and the Mach number at 0.01

With these conditions set, the required mass flow of water is 9 x 10^5 grams per second, and the output area of the diffusor is 8.25 x 10^6 $cm.^2$

7.3 Fuel Separator

The cooling process in the water diffuser cools uranium fuel in the flow well below its melting point. The super-cooled uranium rapidly condenses and forms small droplets and particles which are suspended in the flow.[8] The thermal energy of the flow is used to provide a centrifugal force field to separate the particles from the gas. The drag on these particles is given for Stokes flow as[25]

$$\frac{F_D}{m} = \frac{4.5\mu V}{R_u^2 \rho_u} \qquad (7.3)$$

where μ is the viscosity of the steam, nitrogen mixture. The equation of radial motion of a uranium particle in a centrifugal force field is, with the multiplier of velocity in Equation 7.3defined as C_D,

$$\ddot{r} + C_D \dot{r} - \omega^2 r = 0 \qquad (7.4)$$

This has a solution of the form

$$r = \frac{V_0}{C_D^2 \cdot + 4\omega^2} \left\{ e^{-\frac{C_D + \sqrt{C_D^2 + 4\omega^2}}{2} t} - e^{-\frac{C_D - \sqrt{C_D^2 + 4\omega^2}}{2} t} \right\} \qquad (7.5)$$

For small particles, the drag coefficient C_D is large and the second exponential term of Equation 7.5 decays rapidly regardless of the value of ω and the first term determines the radial position of the particle. For small values of ω, the particle is strongly restrained by the drag forces of the fluid and a centrifugal separator is not very effective. For a centifugal separator to efficiently separate the small particles, the rotational velocity must be at least of the order of the drag coefficient. Under the conditions of the flow just after the water diffusor, the angular velocity must be of the order of 100 radians per second for micron sized particles. This imposes large velocity requirements if the flow is swirled in one section at the outlet of the water diffusor, so the flow is divided into several centrifugal separators.

7.4 Turbines and Pumps

The ideal power available in the flow as it comes out of the uranium separators is given by

$$\mathbb{P} = m_N H_N + m_w H_w \qquad (7.6)$$

It is convenient however to expand the flow only until the water vapor in the flow reaches its saturation point. At this point, the water can be condensed and removed from the flow stream and the nitrogen further cooled to reduce the pump work required to increase its pressure to core entry conditions. Under these conditions Equation 7.6

becomes

$$\mathbb{P} = m_N \left\{ H_N \left(1000^\circ k, (1-\xi) 100 \text{ atm.}\right) - H_N\left(T_{SAT}, \frac{1-\xi}{\xi} P_{SAT}\right)\right\}$$

$$+ m_w \left\{ H_w \left(1000^\circ k, \xi 100 \text{ atm}\right) - H_w\left(T_{SAT}, P_{SAT}\right) \right\} \qquad (7.7)$$

For isentropic expansion of the water vapor, the ideal power available is 2,520 megawatts.

After condensation, the water is pumped as a liquid to 120 atmospheres and injected into the water diffusor. This requires an ideal pump work,

$$W_{P_W} = \overset{\circ}{V}_{OL_W} \, \Delta P_W \qquad (7.8)$$

Ideally, 10.9 megawatts are required for the water pump work.

The nitrogen is cooled in a heat exchanger to 293°K and then pumped back to 1000 atmospheres. This must be done in at least two pumps with interpump cooling to maintain the temperature at or below a structurally safe limit. The ideal nitrogen pump work is given for each pump by

$$W_{P_{N_i}} = m_N \left\{ H_N(T_{2_i}, P_{2_i}) - H_N(T_{1_i}, P_{1_i}) \right\} \qquad (7.9)$$

where the temperatures and pressures are related by the isentropic compression relation

$$\frac{T_{2_i}}{T_{1_i}} = \left(\frac{P_{2_i}}{P_{1_i}}\right)^{\frac{\gamma-1}{\gamma}} \qquad (7.10)$$

The total pump work for all nitrogen pumps is 868 megawatts.

The total heat rejected in the cycle is the sum of the heat of condensation of the water vapor, the cooling of the nitrogen prior to being pumped, and inter-pump cooling after pumping so that the nitrogen can be used to cool the reactor moderator. The total heat rejected in the cycle is 7.1 x 10^3 megawatts.

If water is used as a heat sink for this rejected heat, the mass flow required is

$$m_{rej} = \frac{Q_{rej}}{C_p \Delta T} \qquad (7.11)$$

For a temperature rise of this coolant water of $100^\circ K$, the mass flow required is 1.1 x 10^6 grams per second.

7.5 Minimum Power Level

The minimum operating power level of this test facility is set by the criticality requirements of the reactor, Chapter III, and heat transfer considerations in the reactor and nozzle, Chapter V and VI. This high operating power requires high mass flow rates and large capacity pumps and turbines, as indicated in Section 7.4.

There is no lack of power available to drive this machinery and small units can operate in parallel to provide the desired capacity. As the system is proposed, there is a requirement that the combined efficiency of the turbines and pumps be about 35 percent, but if all of the energy in the cycle is used, efficiencies as low as 12 percent are acceptable.

Equations 5.1 and 6.1 can be combined to express the operating power minimized with respect to the area of the throat,

$$\mathbb{P} = (\epsilon \sigma T_o^4 + .08\, \mathbb{P}/A_c)\, A_c \qquad (7.12)$$

The area of the core is minimized for any pressure and temperature by setting the ratio of nitrogen mass flow to uranium mass flow at 15.4, as was shown in Section 3.2.

Equation 3.11 shows that, with the mass flow ratio fixed, the critical radius, R, varies inversely with the number density of uranium, N_u . For constant operating pressure, the number density of uranium varies inversely with the operating temperature, T_o . The critical radius is then proportional to the operating temperature and the core area is proportional to the square of the operating temperature.

With fixed mass flow ratio and operating pressure, the minimum operating power is, to the first order,

$$P_{min} = C\, T_o^6 \qquad (7.13)$$

where C is a proportionality constant.

Equation 7.13 is valid only in the temperature range where the heat loads to the moderator are too large to be removed by conventional cooling and the energy absorbed in protecting the moderator walls must pass through the nozzle.

A plot of the estimated minimum operating power as a

function of temperature is given in Figure 11. At operating temperatures below 7000°K, this facility is in the power category of large arc tunnels and MHD devices, and the relative merits of each type of facility would have to be considered before deciding which system is most desirable. At the higher temperatures at which this facility is conceptionally most useful, the minimum operating power rises rapidly, as well the size of the physical plant. It is also noted that reducing the operating temperature reduces the re-entry simulation capability of the test facility, as illustrated in Figure 2.

The economics of developing such a facility must be examined to determine if the need for such a testing capability justifies the expense of so large an undertaking.

CHAPTER VIII

CONCLUSIONS

Within the scope of the material examined in this report it appears to be within the capability of projected technology to design and build a high enthalpy test facility powered by a gaseous core reactor.

This test facility can not exactly duplicate all of the conditions imposed upon a vehicle during an atmospheric re-entry, but does provide a means of testing re-entry materials and shapes under the high temperature and shear conditions which are encountered during a re-entry. Existing facilities cannot attain the high temperature, high pressure, long duration flows necessary to test the shear mode of failure. The gaseous core reactor provides the power required for these flows.

Nuclear contamination of several proposed re-entry materials is slight enough so that the model may be examined immediately after a test run. This may not be true in general and each proposed test material must be examined by the methods of Chapter IV to determine the degree of contamination.

The high neutron absorption cross section of nitrogen as a working fluid causes the reactor to be large and the mass flow ratio of uranium to nitrogen to be relatively

high. The reactor size and operating power is minimized by setting the mass ratio of nitrogen to uranium in the core at 15.4 to 1. This adversely affects the quality of the mixture for simulating atmospheric conditions, but is slight enough to be considered acceptable.

The minimum operating power of the test facility is set by the radiant power of the core which cannot be absorbed by the moderator and must pass through the nozzle. In the neighborhood of 10,000 °K, for a constant mass ratio, the minimum operating power varies as the temperature in the core to the sixth power and as the inverse of the core pressure.

Operation of the facility at the minimum power level requires high mass flow rates and associated high capacity pumps and turbines. These pumps must be capable of high pressure and high pressure ratio operation. Efficiency of the combined turbine and pump can be as low as twelve percent for self sustaining operation of the system.

The turbo-machinery required set a practical upper limit on the operating power of the system. Structural considerations impose an upper pressure limit on the system.

This analysis has examined only the minimum powered point for the operation at the maximum pressure and temperature and has found that such a facility appears technically feasible. Operation of a facility at lower power levels is possible with a reduction in chamber temperature and associated loss of re-entry simulation capability.

It is recommended that the economics involved in the construction, maintenance and operation of this system be examined to determine if such a large facility would be economically practical.

TABLE I

FISSION PRODUCTS

Radionuclide	Half Life	Yield Fraction	Decay Constant
A	$t_{1/2}$(sec)	η_A	λ_A (sec^{-1})
Br^{87}	55.6	10^{-3}	1.2×10^{-2}
Br^{89}	4.51	5×10^{-3}	1.54×10^{-1}
Ag^{110}	24.2	10^{-4}	2.9×10^{-2}
In^{114}	72	10^{-4}	9.6×10^{-3}
In^{116}	13	10^{-4}	$5.\overset{3}{4} \times 10^{-2}$
Sb^{135}	1.52	4×10^{-2}	4.56×10^{-1}
I^{137}	22	6×10^{-2}	3.1×10^{-2}

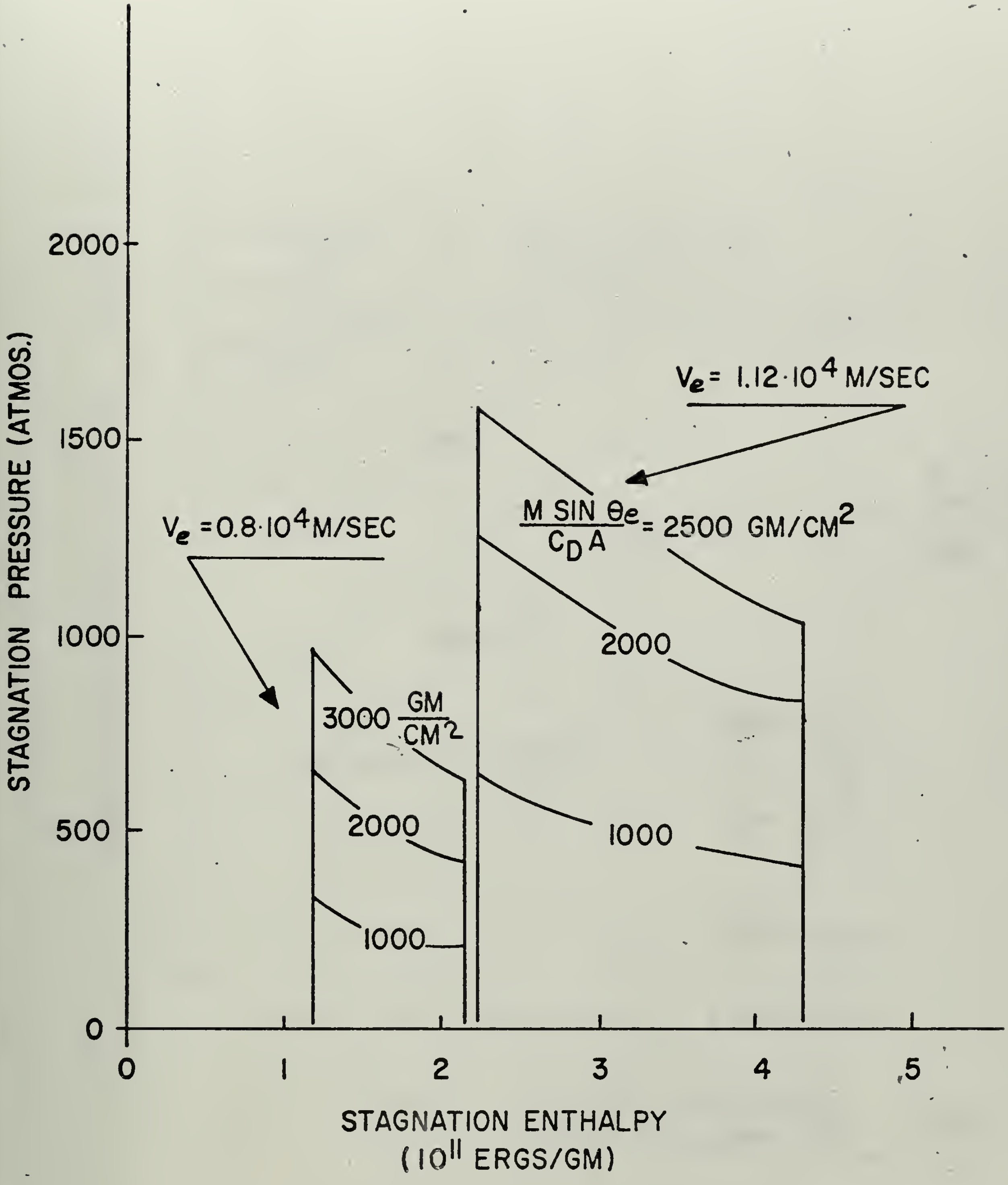

FIGURE I REENTRY STAGNATION PRESSURE AND ENTHALPY.

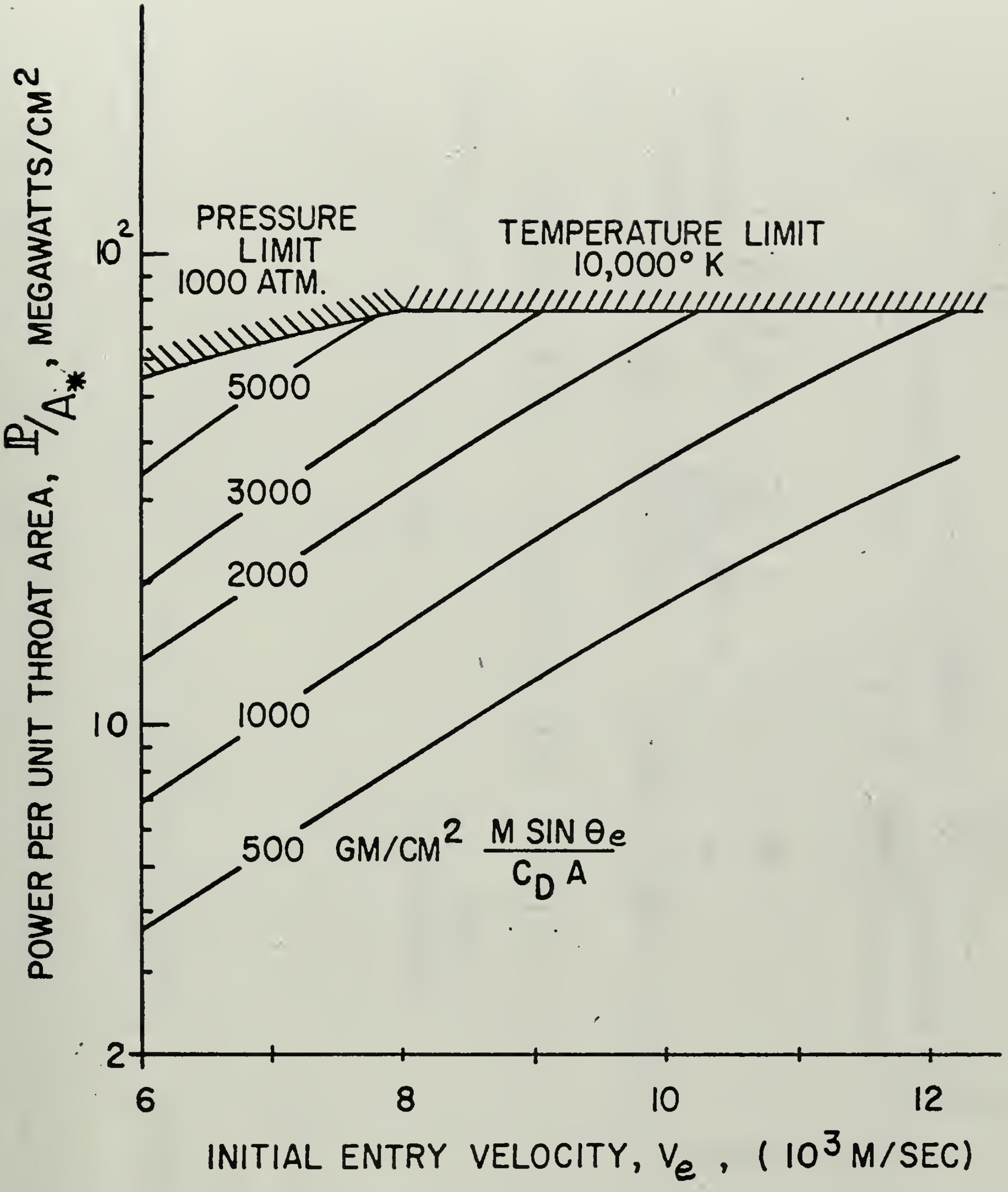

FIGURE 2 REENTRY SIMULATION POWER REQUIREMENTS.

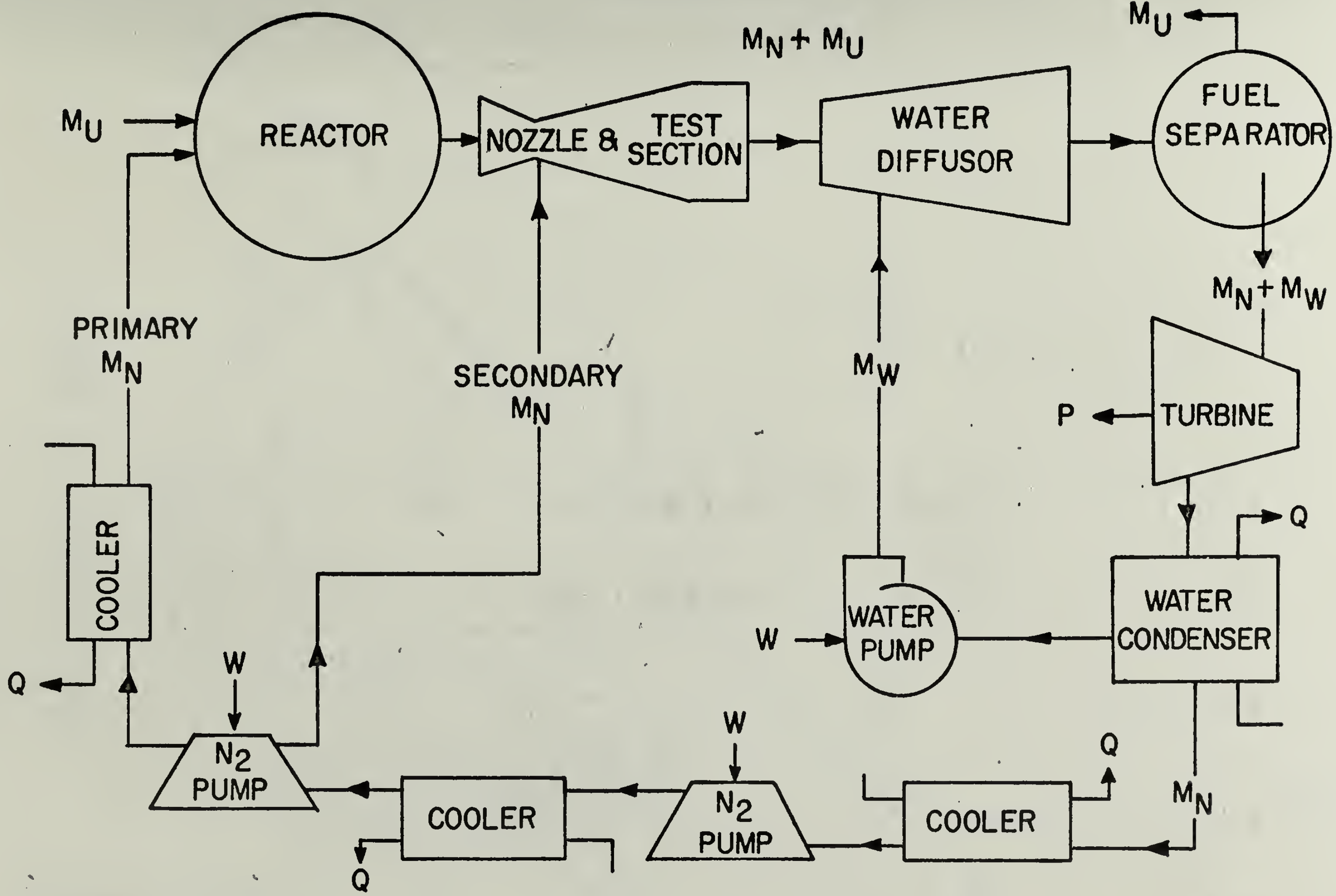

FIGURE 3 TEST FACILITY SCHEMATIC.

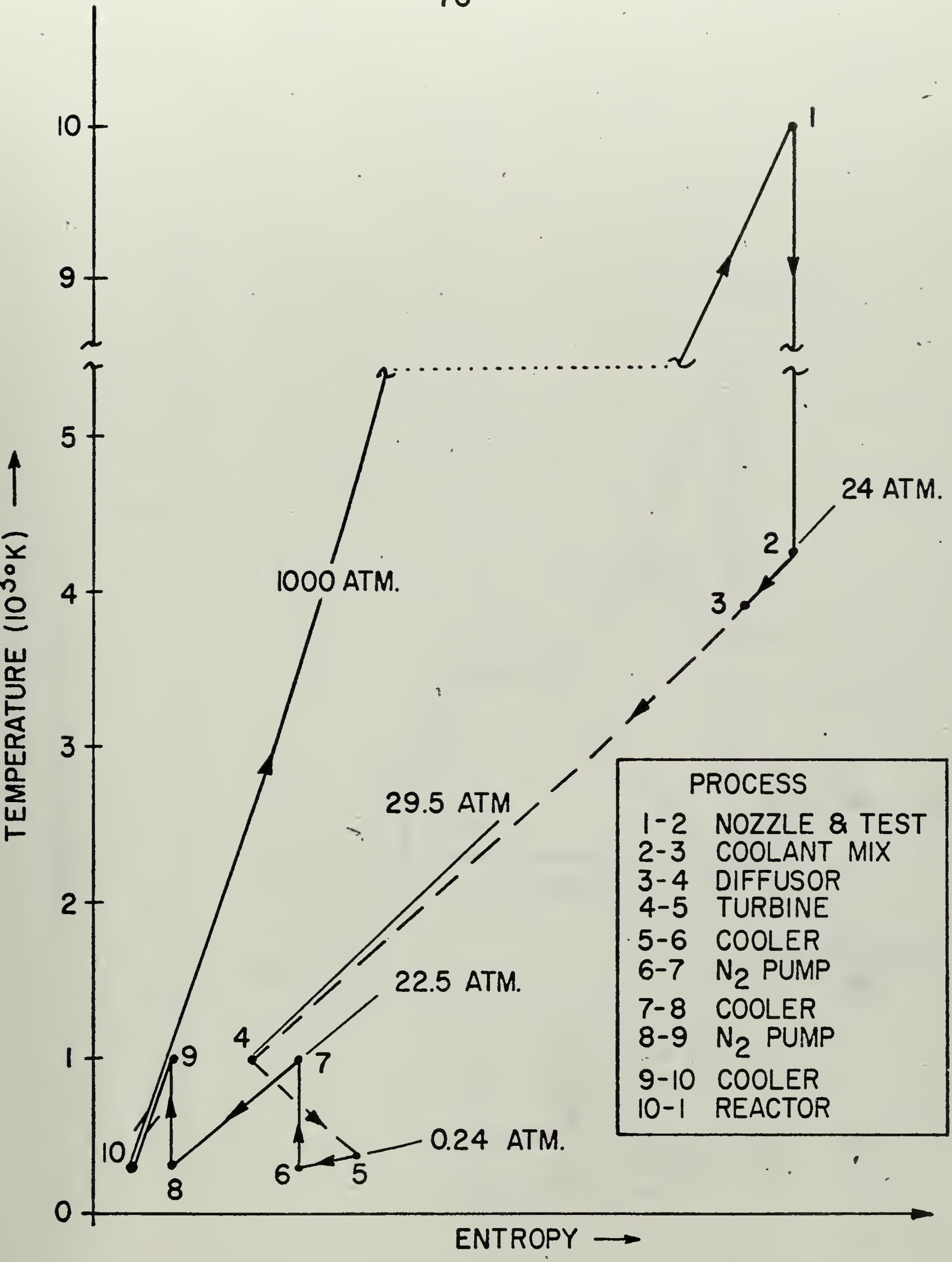

FIGURE 4 NITROGEN CYCLE.

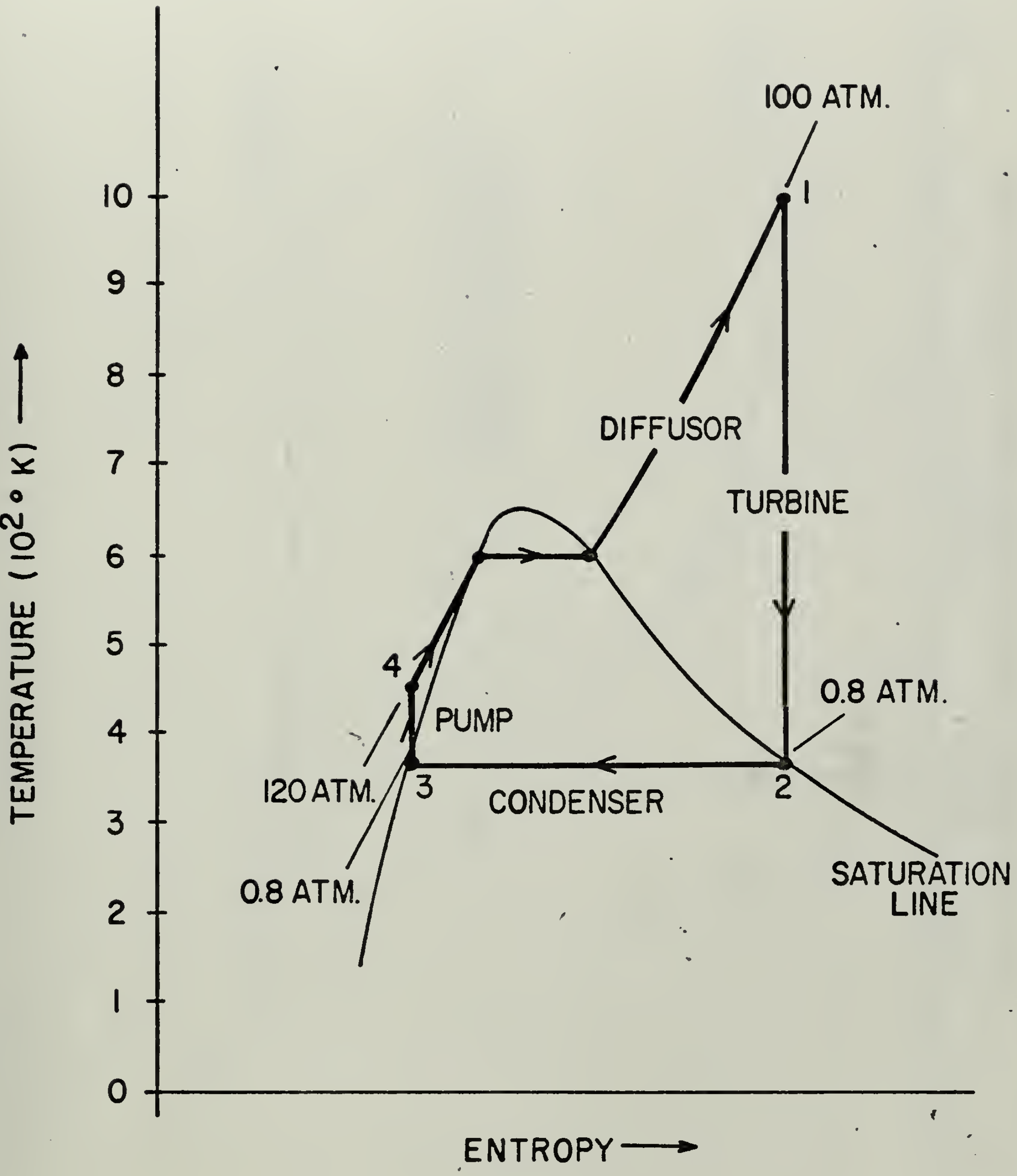

FIGURE 5 WATER CYCLE.

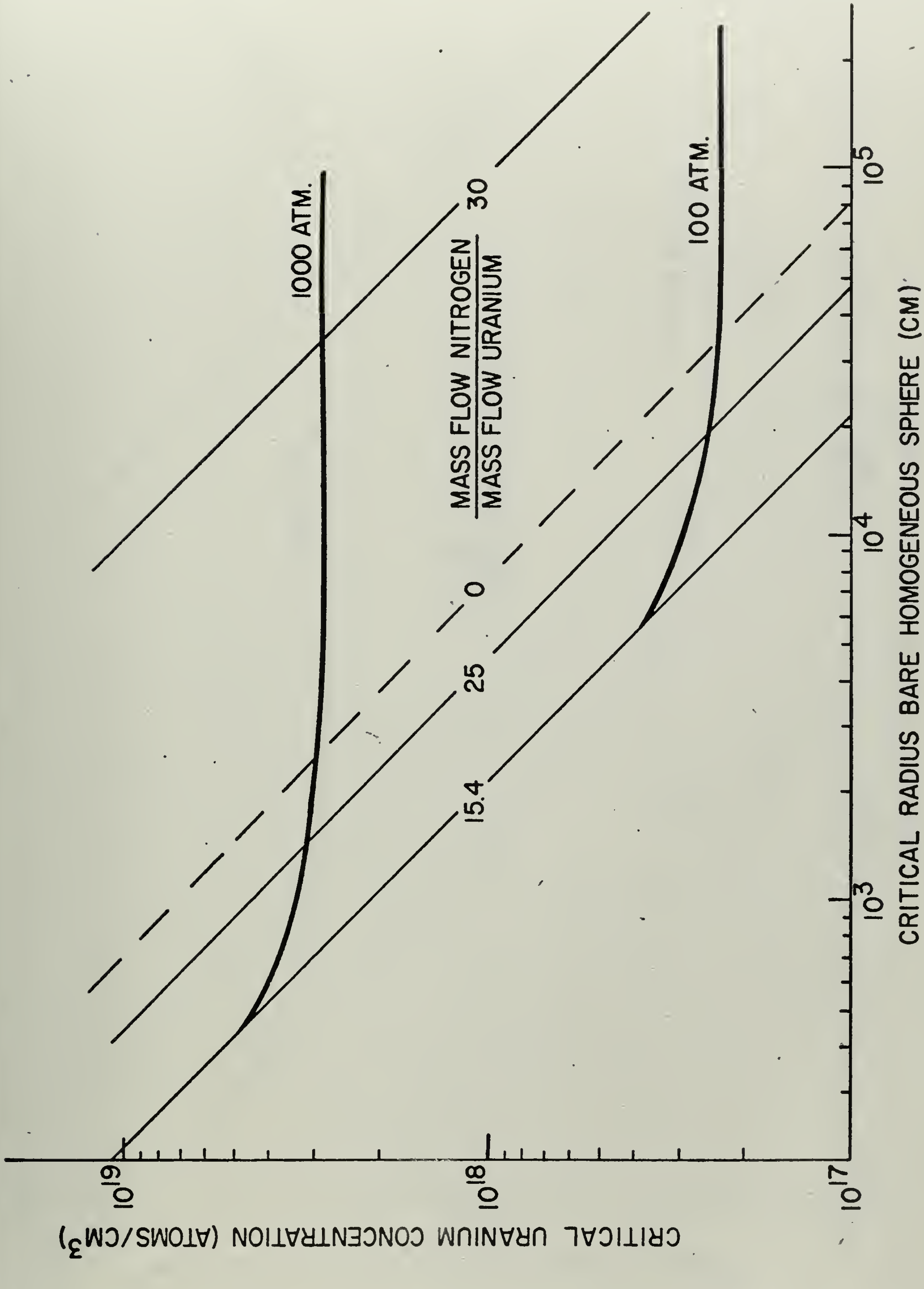

FIGURE 6 CRITICALITY OF BARE URANIUM–NITROGEN GASEOUS REACTOR.

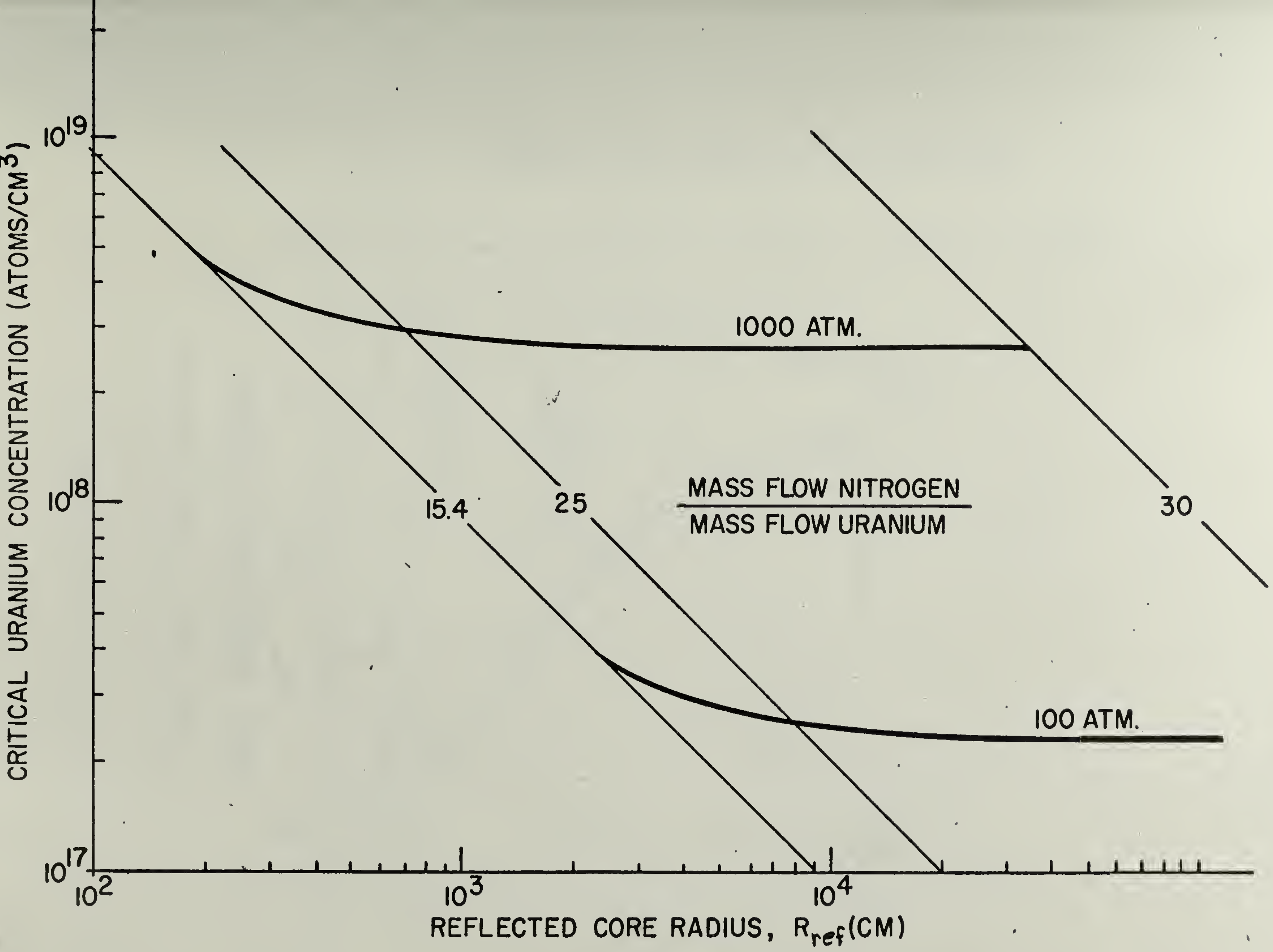

FIGURE 7 CRITICAL RADIUS OF BERYLLIUM REFLECTED URANIUM–NITROGEN GASEOUS REACTOR.

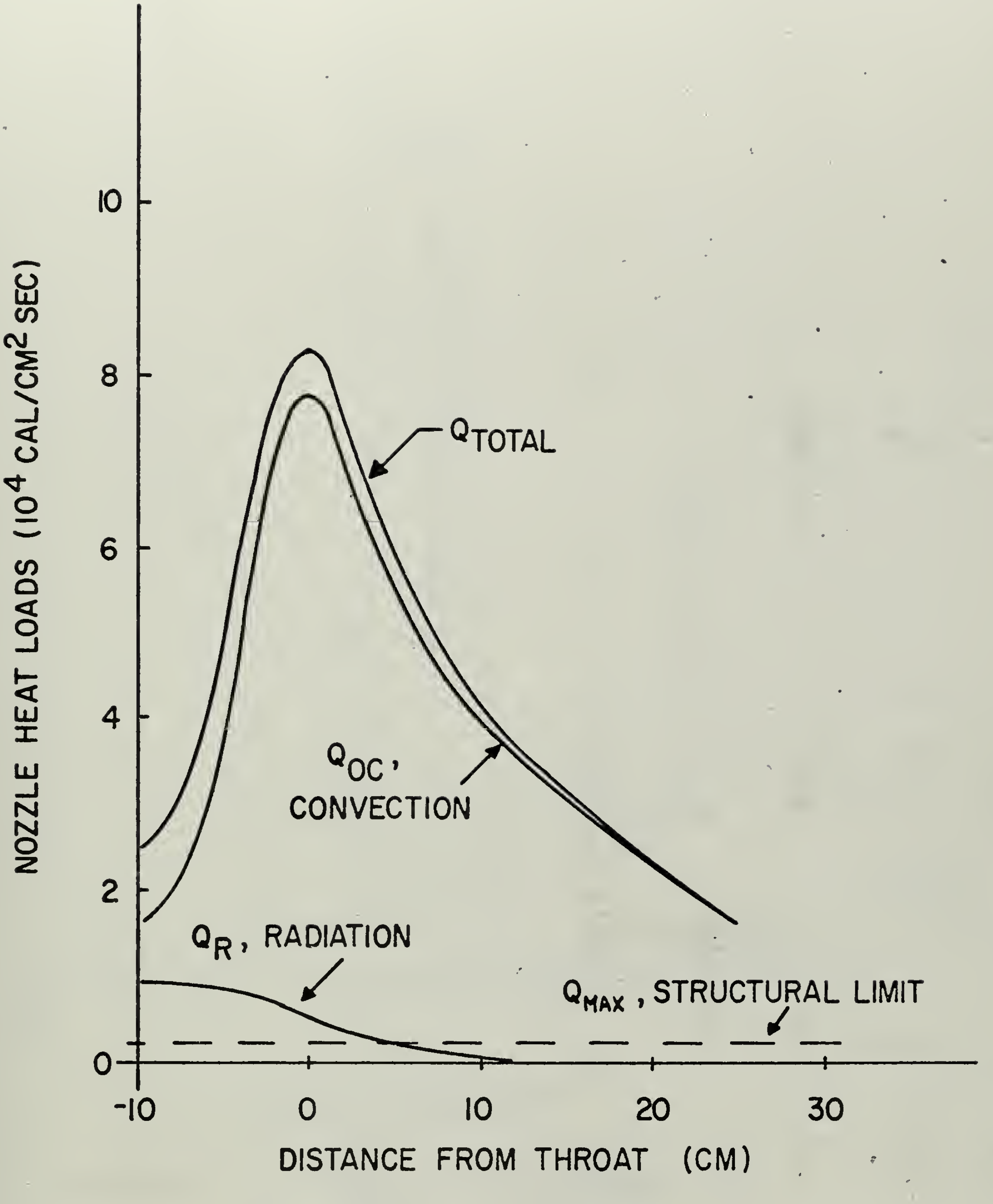

FIGURE 8 NOZZLE HEAT LOADS.

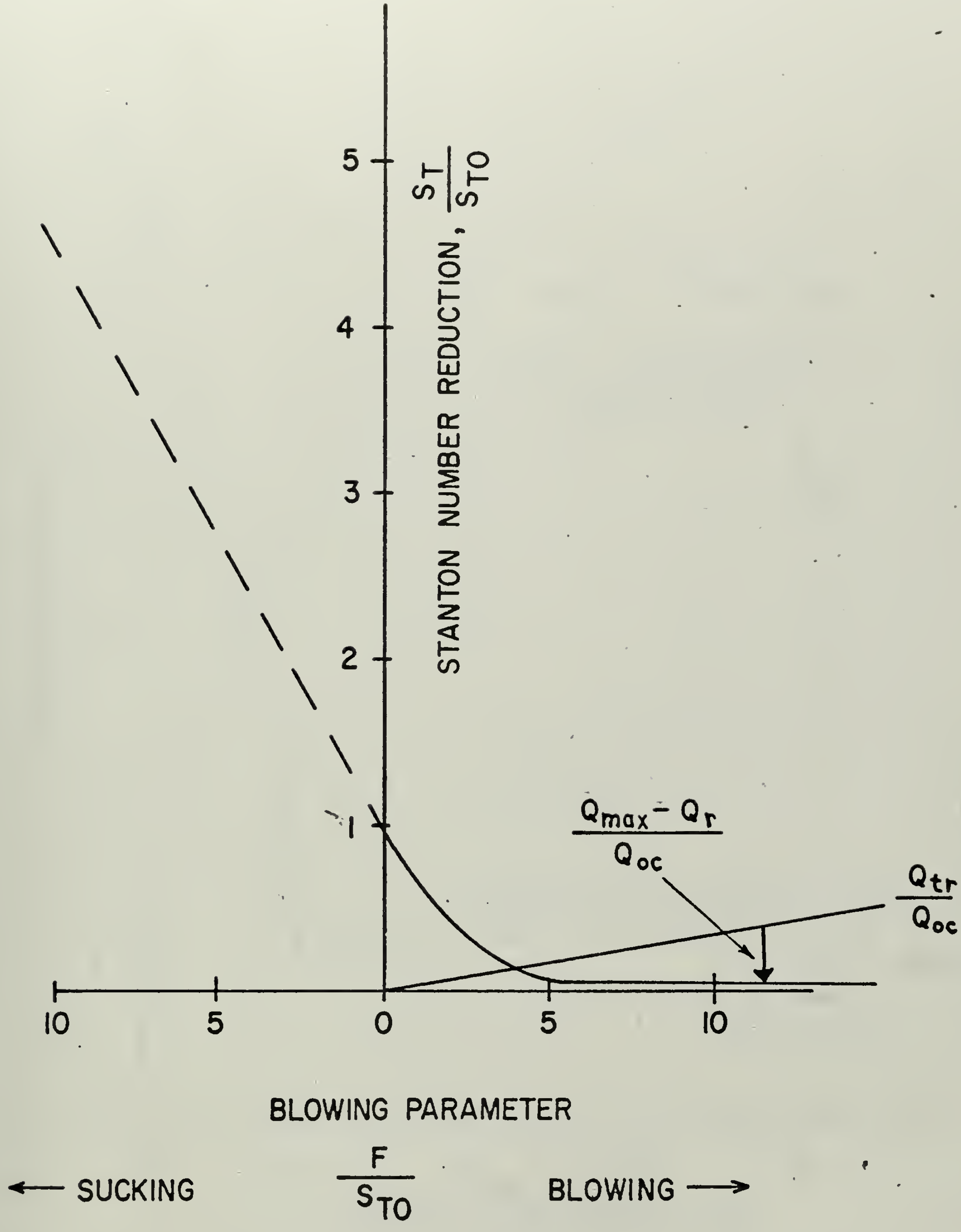

FIGURE 9 TRANSPIRATION COOLING REQUIREMENT.

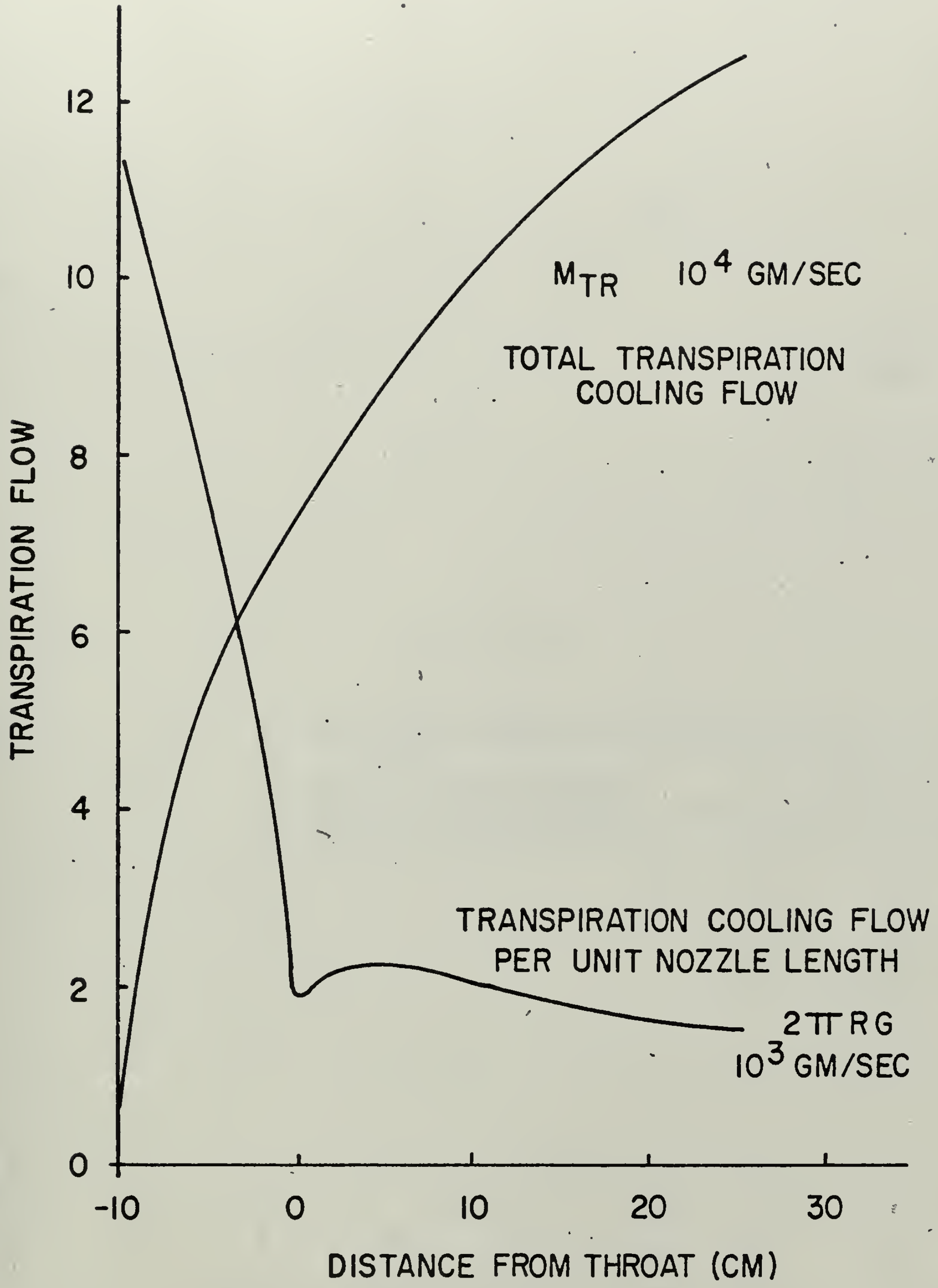

FIGURE 10 NOZZLE TRANSPIRATION FLOW.

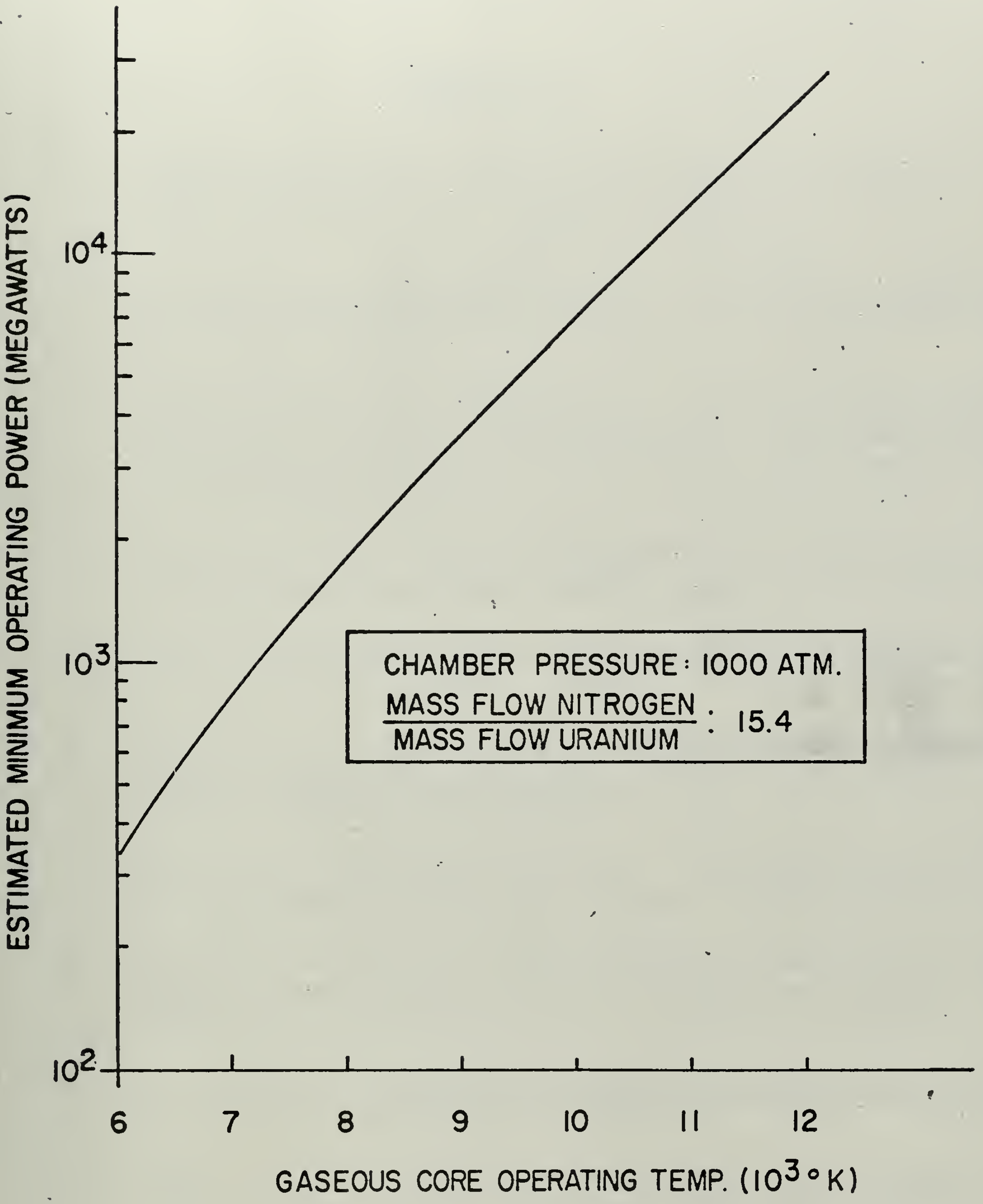

FIGURE 11 MINIMUM OPERATING POWER FOR GASEOUS CORE REACTOR.

REFERENCES

1. Eggers, A.J., Jr. " The Possibility of a Safe Landing ", Space Technology, Chapter 13, Seifert, H.S., Ed., Wiley and Sons, Inc., London, (1959)

2. Grunstfest, I. and Shenker, L., " Ablation ". Modern Science and Technology, Colborn, R., Ed., Van Nostrand Co., N.J. (1965)

3. Tazzilli, R.A. and Ramke, W G., " Evaluation of Graphite Composites in Re-Entry Environments ", AIAA/ASME Seventh Structures and Materials conference, Cocoa Beach, Fla., (April 18-20, 1966)

4. Stadler, J.R., " Re-Entry Simulation ", XVII International Astronautics Conference, Madrid, Spain, (Oct. 9-15, 1966)

5. Pope, A. and Goin, K.L., High Speed Wind Tunnel Testing, Wiley and Sons, London, (1965)

6. Mills, C.B. " Criticality ", Proceedings of an Advanced Nuclear Propulsion Symposium, Cooper, R.S., Editor USAEC Contract W-7405-ENG.36

7. Duke, E.E., and Houghton, W.J., " Gaseous Fueled Nuclear Rocket Engine", AIAA Paper 66-621, (June 1966)

8. Hunter, H., et. al., "Recirculating, Coaxial Flow Gaseous-Core Nuclear Reactor Concept ", AIAA Paper 66-618, (June 1966).

9. Glasstone, S., Principles of Nuclear Reactor Engineering, Van Nostroand Co., N.J., (1958)

10. Bartz, D.R., " An Approximate Solution of Compressible Turblent Boundary Layer and Convective Heat Transfer in Convergent-Divergent Nozzles " Jet Propulsion, 27, (1957)

11. Kramer, E.L. and Gronich, S., "A Transpiration Cooled Nozzle as Applied to a Gas-Core Nuclear Propulsion System," JSR, 2, 3, (May-June 1965)

12. Howell, J.R. and Renkel, H.E., "Analysis of the Effects of a Seeded Propellant Layer on Thermal Radiation in the Nozzle of a Gaseous Core Nuclear Propulsion System" NASA TN D)-3119, (December 1965)

13. Lanzo, C.H. and Ragsdale, R.G., "Experimental Determination of Spectral and Total Transmissivities of Clouds of Small Particles." NASA TN D-1405 (September 1962)

14. Ahtye, W.F. and Peng, T.C., "Approximations for the Thermodynamic and Transport Properties of High Temperature Nitrogen with Shock Tube Applications.", NASA TN D-1303, (July 1962)

15. Landau, H.G., "Heat Conduction in a Melting Solid", Quarterly of Applied Mathematics, 8, 1, (1950)

16. Hertzberg, A., et. al., " A Summary of Shock Tunnel Development and Application to Hypersonic Research," CAL AD-1052-A-12 (July 1961)

17. Fabian, G.J., " Hypersonic Research Summary " CAL AD-1118-A-11 (June 1960)

18. Bussard, R.W. and DeLaver, R.D., Fundamentals of Nuclear Flight, McGraw-Hill Co., N.Y., (1965)

19. Hughes, H., Neutron Cross Sections, BNL 325, Brookhaven National Laboratory, N.Y.

20. Stephenson, R., Introduction to Nuclear Engineering, Second Edition, Mc Graw-Hill, N.Y. (1958)

21. National Committee on Radiation Protection and Measurement, "Permissible Levels of Radiation Exposure to Man", AEC Appendix 0524-02-A,Congress of the US, (May 1966)

22. National Bureau of Standards, Nuclear Data, NBS Circular 499, (1950).

23. Kendrick, J.B., Editor, TRW Space Data, TRW Systems Group, TRW Inc., (1967)

24. Mason, N. H., Chairman, Material Properties Handbook, NATO ARGARD Structures and Materials Panel, (May 1966)

25. Rohsenow, W H. and Choi, N Y., Heat Mass and Momentum Transfer, Prentice Hall, N.J., (1963)

26. Keenan, J.H. and Keys, F.G., Thermodynamic Properties of Steam, Wiley and Sons Inc., N.Y. (1963)

thesF527
A high enthaply i.e., enthalpy test fa
3 2768 001 96814 2
DUDLEY KNOX LIBRARY